

NASA Technical Memorandum 87805

# Analytical Caustic Surfaces

R. F. Schmidt

APRIL 1987

**NASA**

**CONTENTS**

ABSTRACT . . . . .	v
NOTATION . . . . .	vii
INTRODUCTION . . . . .	1
CENTER SURFACES . . . . .	7
CAUSTICS FROM DISTORTED WAVEFRONTS . . . . .	11
CAUSTICS FROM FLUX DENSITY SINGULARITIES . . . . .	14
CAUSTICS FROM A TENSOR ALGORITHM . . . . .	24
CONCLUSION . . . . .	27
ACKNOWLEDGMENTS . . . . .	28
REFERENCES . . . . .	29
APPENDIX A – Gauss/Seidel Aberrations (Parallel Distortion of Gaussian Wavefront) . . . . .	31
APPENDIX B – Gauss/Seidel Aberrations (Normal Distortion of Gaussian Wavefront) . . . . .	33
APPENDIX C – The Caustic Surfaces of a Paraboloid and Inclined Plane Wave . . . . .	39

**PRECEDING PAGE BLANK NOT FILMED**

## NOTATION

EV	Evolute
INV	Involute
$\Lambda$	Wavefront
$\Omega$	Caustic surface of two branches ( $\omega_1, \omega_2$ )
$\bar{S}_i, \bar{S}_r$	Incident and reflected rays
$\bar{N}$	Normal to a surface
LC <sub>1</sub> , LC <sub>2</sub>	Lines of curvature
$\bar{e}_1, \bar{e}_2$	Characteristic directions (eigenvectors on a wavefront)
$k_1, k_2$	Characteristic values (eigenvalues), principal normal curvatures
$K_N, K_G, K_M$	Normal, Gaussian, and mean curvatures
$x = (x, y, z)$	Generic parametric surface coordinates
$\bar{x}_u, \bar{x}_v$	Tangents to a surface
$\bar{x}_{uu}, \bar{x}_{uv}, \bar{x}_{vv}$	Tangent rates
E, F, G	Coefficients of the First Fundamental Form
e, f, g or L, M, N	Coefficients of the Second Fundamental Form
$\lambda_i$	Coefficients associated with $k_i, e_i$
$\alpha$	Azimuthal angle in Euler's Theorem
$\bar{N}_u, \bar{N}_v$	Derivatives in Rodrigues' formula
R <sub>21</sub> , R <sub>22</sub>	Principal normal radii of curvature (Flux-density context)
$F_{dS_1-dS_2}$	Flux-density
$\phi_i, \psi_i$	Angles of incidence on deflector and receiver
$a_0, a_1, a_2$	Coefficients of the Flux-density formula
$r_2$	Distance from reflector to observer (Flux-density formula)
F	Focal length of a paraboloid
$\gamma$	Reflector surface
$\delta_\Lambda$	Wavefront aberration along normal to Gaussian sphere (GS)
$\delta_\gamma$	Reflector distortion
OPL	Optical path length
$\Pi_1, \Pi_2, \Pi_3$	Planes associated with a Darboux frame
$C_1, C_2$	Centers of curvature
$\Gamma_1, \Gamma_2$	Edges of regression (space curves)
$\omega_{2l+n}, \omega_{2m+n}, n$	Aberration coefficients
$I_1, I_2, I_3$	Optical invariants ( $h^2, \sigma^2, h \sigma \cos \zeta$ )
$\zeta$	Azimuthal variable
$\sigma$	Radial variable
c	Radius of Gaussian sphere

PRECEDING PAGE BLANK NOT FILMED

## ANALYTICAL CAUSTIC SURFACES

### INTRODUCTION

The study of caustic surfaces is rooted in antiquity. "One of the earliest discoveries in optics (F. Maurolycus, 1575) was that the rays of a normal system are tangential to a surface, the so-called caustic surface, and that the general ray is tangential to the caustic surface in two points," Ref. 1, p. 156. The study of caustic surfaces persists to the present. "Thom himself observed that a usual interpretation of his theorem on the classification of singularities of gradient mappings as elementary catastrophes were the so-called caustics." Ref. 2 (1982), p. 1080. A great amount of material on caustics can be found between the discoveries of Maurolycus and the observation of Thom. Many statements pertaining to caustics stir the imagination; some are provocative. For example, the caustic has been described as "a zero, one-, or two-dimensional manifold in every neighborhood of which more than one ray of any infinitesimal tube of the field passes through some point," Ref. 3, p. 326. In geometrical optics: "The envelope to a family of rays reflected from some surface is called a caustic, and the Hilbert integral along an envelope degenerates into a variational integral," Ref. 4, p. 79. From differential geometry: "The center surfaces are the loci of the centers of principal (normal) curvature on the surface," Ref. 5, p. 94. The caustic surfaces are usually associated with focusing, Ref. 6, p. 259.

The objectives of this document are limited to a discussion of several alternative means for obtaining analytical caustic surfaces and the exploration of wavefronts and caustics of a general form that derives in a natural way via aberration theory. An overall appreciation of the structure of this document may be obtained from Figure 1. A family of lines defining the caustic surfaces is obtained analytically from rays via the law of reflection, perhaps the simplest and most familiar approach. Introduction of the optical path length, in conjunction with the law of reflection, leads to the wavefront approach. Procedures based on differential geometry permit the analytical development of center surfaces, or caustic surfaces, as a set of points via wavefront normals and principal normal curvatures ( $k_1, k_2$ ). A flux-density algorithm obtains an equation for the caustic surfaces in terms of the intrinsic Gaussian, mean, and normal curvatures ( $K_G, K_M, K_N$ ) of a reflector by exploiting a singularity of the formulation. This approach allows the mapping of contours of equal flux density and the imbedding of the caustic surfaces. A second method that leads to parametric equations of the caustic surfaces uses a tensor algorithm that regards only the source and the reflector, to the exclusion of the wavefront.

The practical or applications aspect of "Analytical Caustic Surfaces" is implicitly contained in Figure 1. It can be seen that provision is made for a distortion of the reflector, resulting in a distorted wavefront. Alternatively, an idealized wavefront may be assumed at the outset, and caustic surfaces may be obtained after superimposing combinations of many types of appropriately weighted classical wavefront aberrations. Sources ( $\bar{S}_i$ ) may be generalized to represent converging, diverging, or planar types, and superposition of sources is allowed under the flux density algorithm. Intermediate media, between source and reflector, may be treated as a modification of the illumination block of Figure 1.

The relationship between rays, wavefronts, and caustics is illustrated for convenience in two dimensions in Figure 2 and initial discussion is in terms of involutes and evolutes. Actually, the latter are defined for space curves in three dimensions as follows:

- (1) The evolute of a curve is the geometric locus of the centers of curvature of a curve. Ref. 7, p. 58  
and
- (2) The involute of a curve lies in the tangent surface of that curve and intersects the tangent lines orthogonally. Ref. 8, p. 84.

Rays are seen to be orthogonal to wavefronts and tangent to the caustic curve. The arc distance  $S_{12}$  on the caustic equals the tangent distance from the wavefront to the caustic. It is therefore the inverse of the curvature at every point of the wavefront. The evolute of the wavefront is the caustic. The involute of the caustic is the wavefront. The wavefront is not unique and depends on the choice of an initial point of the caustic. Bertrand curves are recalled. Ref. 8, p. 98

$$EV(\Lambda) = \Omega \quad (1)$$

$$INV(\Omega) = \Lambda \quad (2)$$

Generation of Figure 2 is made easy since the caustic ( $\Omega$ ) was taken to be a circle for which a closed-form expres-

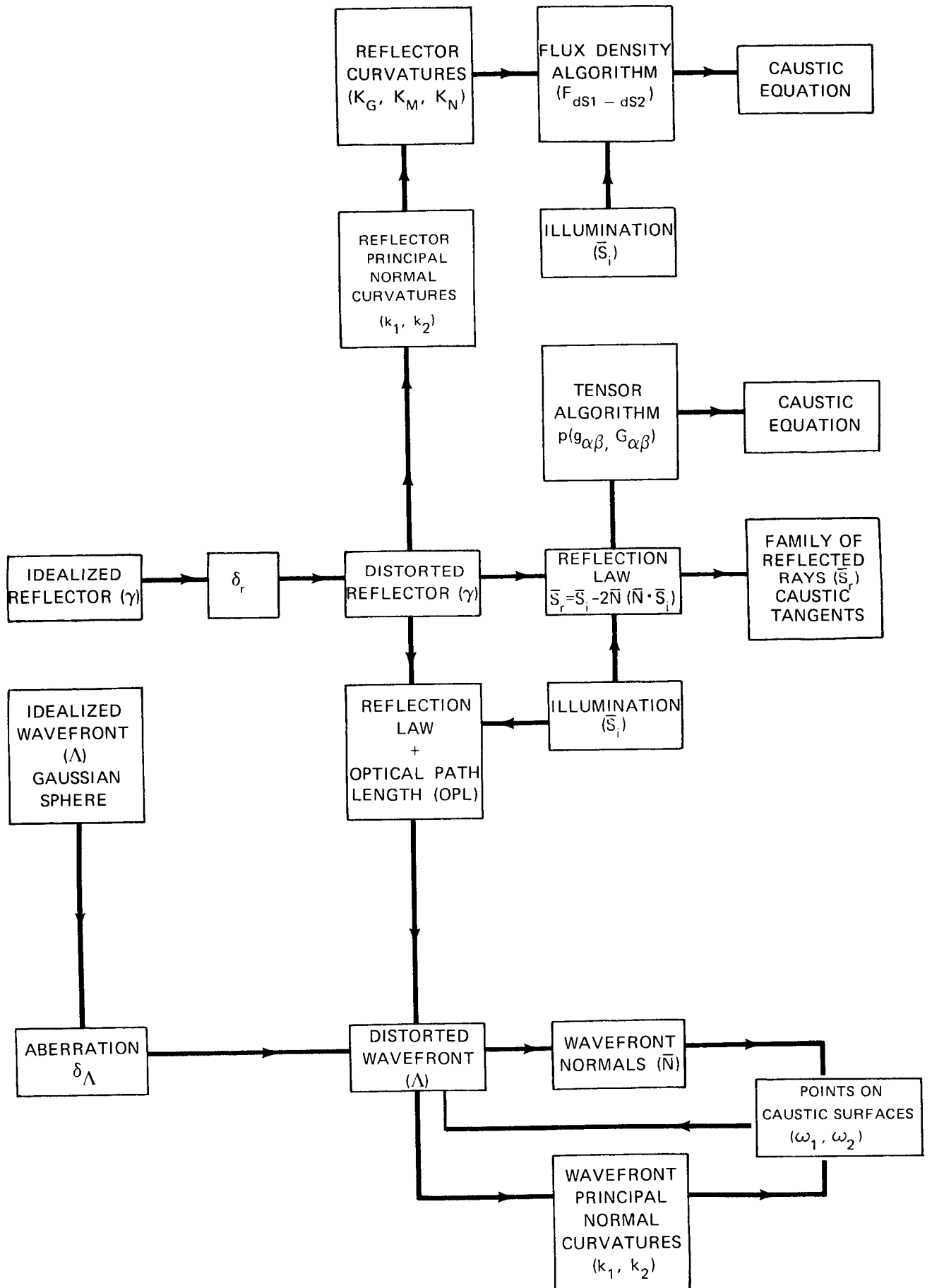


Figure 1. Analytical Caustic Surfaces.

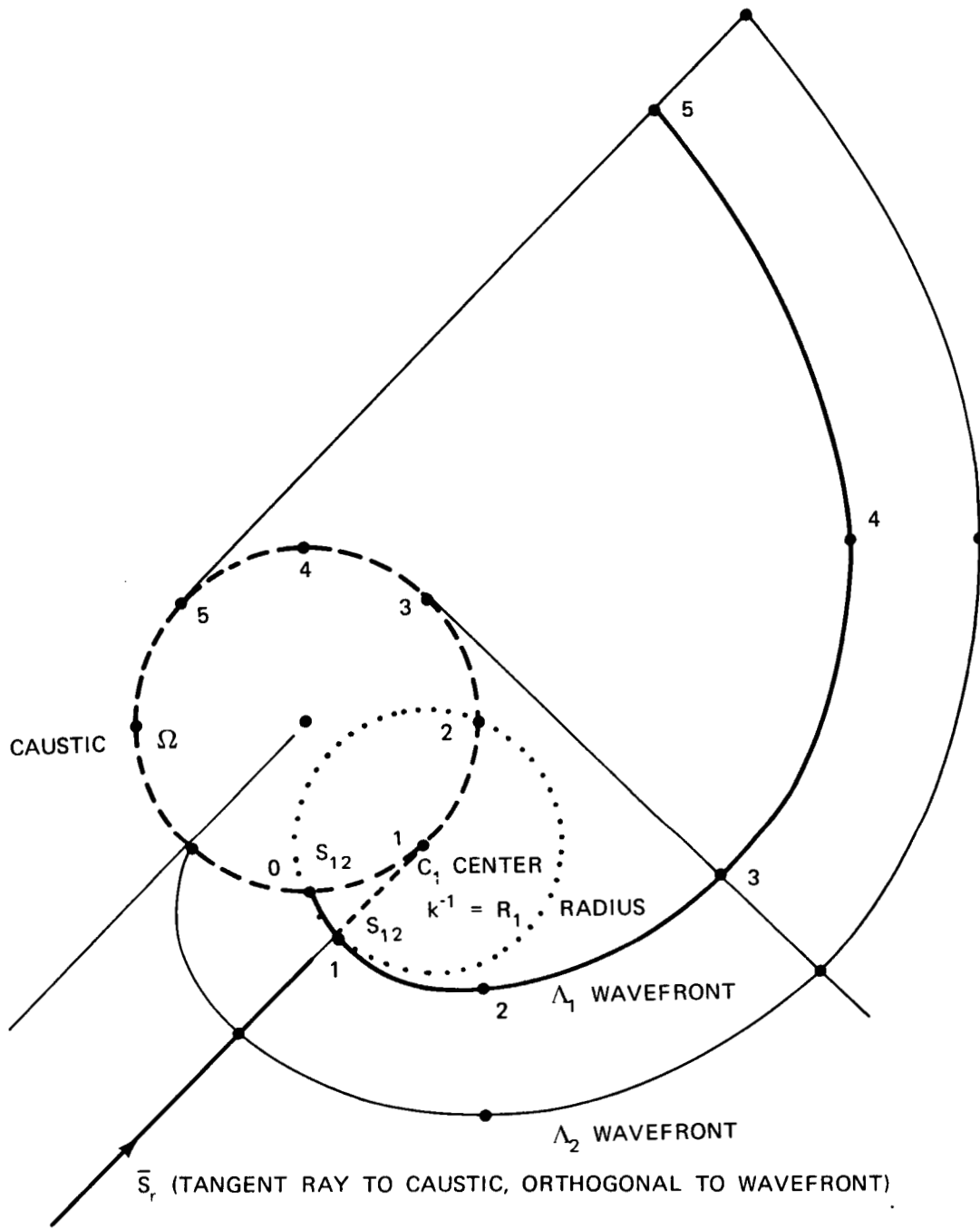


Figure 2. Rays, wavefronts and caustics.

sion of arc length is available. This in turn provides the radii of curvature of  $\Lambda$  directly. The example is a particularly good one since a portion of the Tschirnhausen cubic is nearly circular. The latter curve is a cross-section of the caustic surface for off-axis plane-wave incidence on a parabolic arc. Background material on the derivation of this cubic curve is found in Ref. 9 and Ref. 10. Figure 3 illustrates the formation of Tschirnhausen's cubic by tangent rays and is a point of departure for developing analytical three-dimensional caustic surfaces of paraboloids and other reflectors under various assumptions regarding illumination and distortion.<sup>1</sup>

The objectives of this document are brought out in greater detail in Figure 4. Representative wavefronts ( $\Lambda$ ) and their associated center or caustic surfaces ( $\omega_1, \omega_2$ ) are shown without any reflector surface ( $\gamma$ ) or illuminating rays ( $\bar{S}_i$ ). Since the system of the reflected rays ( $\bar{S}_r$ ) is orthogonal to the wavefront ( $\Lambda$ ), the wavefront normals and the reflected rays are co-directional or at most anti-directional. The rays ( $\bar{S}_r$ ) are tangent to the caustic branches ( $\omega_1, \omega_2$ ). An analytical means of determining the caustic surfaces may therefore be reduced to the problem of finding the wavefront normals ( $\bar{N}$ ), a family of lines in three-dimensional space. Alternatively, the caustics may be found as a set of points, using the definition of a center surface, if the extrema ( $k_1, k_2$ ) of normal curvatures ( $k$ ) can be found at every point  $P$  on the wavefront  $\Lambda$ . Standard methods of differential geometry are employed to obtain both the unit normals ( $\bar{N}$ ) to a surface ( $\bar{x}$ ), via the un-normalized tangents ( $\bar{x}_u, \bar{x}_v$ ), and the principal normal curvatures ( $k_1, k_2$ ). These methods also permit the writing of equations, practical closed-form expressions, to describe the caustic surfaces analytically in many cases. An advantage of obtaining the caustic surface equations is that they may in turn be analyzed for curvature.

An objective of this document is to include wavefront aberrations and pursue the analysis when the tangents  $\bar{x}_u$  and  $\bar{x}_v$  are no longer orthogonal, and all terms of the first and second fundamental forms of differential geometry are different from zero. The directions of the principal lines of curvature ( $LC_1, LC_2$ ) imply orthogonal vectors (eigenvectors) associated with the principal normal curvatures (eigenvalues) and principal centers of curvature ( $C_1, C_2$ ) in Figure 4. The vectors  $\bar{N}, \bar{e}_1, \bar{e}_2$  then constitute an orthogonal moving triad on the wavefront ( $\Lambda$ ), and the pairs of vectors ( $\bar{N}, \bar{e}_1$ ), ( $\bar{N}, \bar{e}_2$ ) identify with (principal) planes of curvature.<sup>2</sup> All of the preceding discussion pertains to the formation of caustic surfaces from a wavefront using standard methods of differential geometry to obtain the characteristic values ( $k_1, k_2$ ) and the normal ( $\bar{N}$ ) of the latter surface.

Similar techniques may be applied directly to a reflector surface instead of a wavefront to obtain the caustic surfaces. Characteristic values and surface normals are required as before. The stipulation of an incident ray ( $\bar{S}_i$ ) and the reflector normal ( $\bar{N}$ ) defines a plane of curvature intersecting the reflector and therefore a normal curvature ( $K_N$ ), not necessarily a principal normal curvature. The characteristic values ( $k_1, k_2$ ) of the reflector determine the Gaussian ( $K_G$ ) and mean ( $K_M$ ) curvatures. An existing analysis, predicated on these intrinsic curvatures ( $K_G, K_M, K_N$ ) of the reflector, provides both flux density and caustic information through exploitation of a singularity of the formulation, as mentioned, previously. Standard methods of differential geometry may therefore be used in conjunction with alternative theories for obtaining caustic surfaces.

<sup>1</sup> Once the nodal cubic has been identified it may be rewritten in parametric form as

$$x = 3a(t^2 - 3), \quad y = at(t^2 - 3),$$

from which the expression for arc-length,

$$S = at(t^2 + 3)$$

follows.

<sup>2</sup> The triad is called a Darboux frame for surfaces, and is the analogue of Fresnel's frame ( $\bar{t}, \bar{n}, \bar{b}$ ) for space curves. Ref. 14, p. 210; Ref. 5, p. 261.

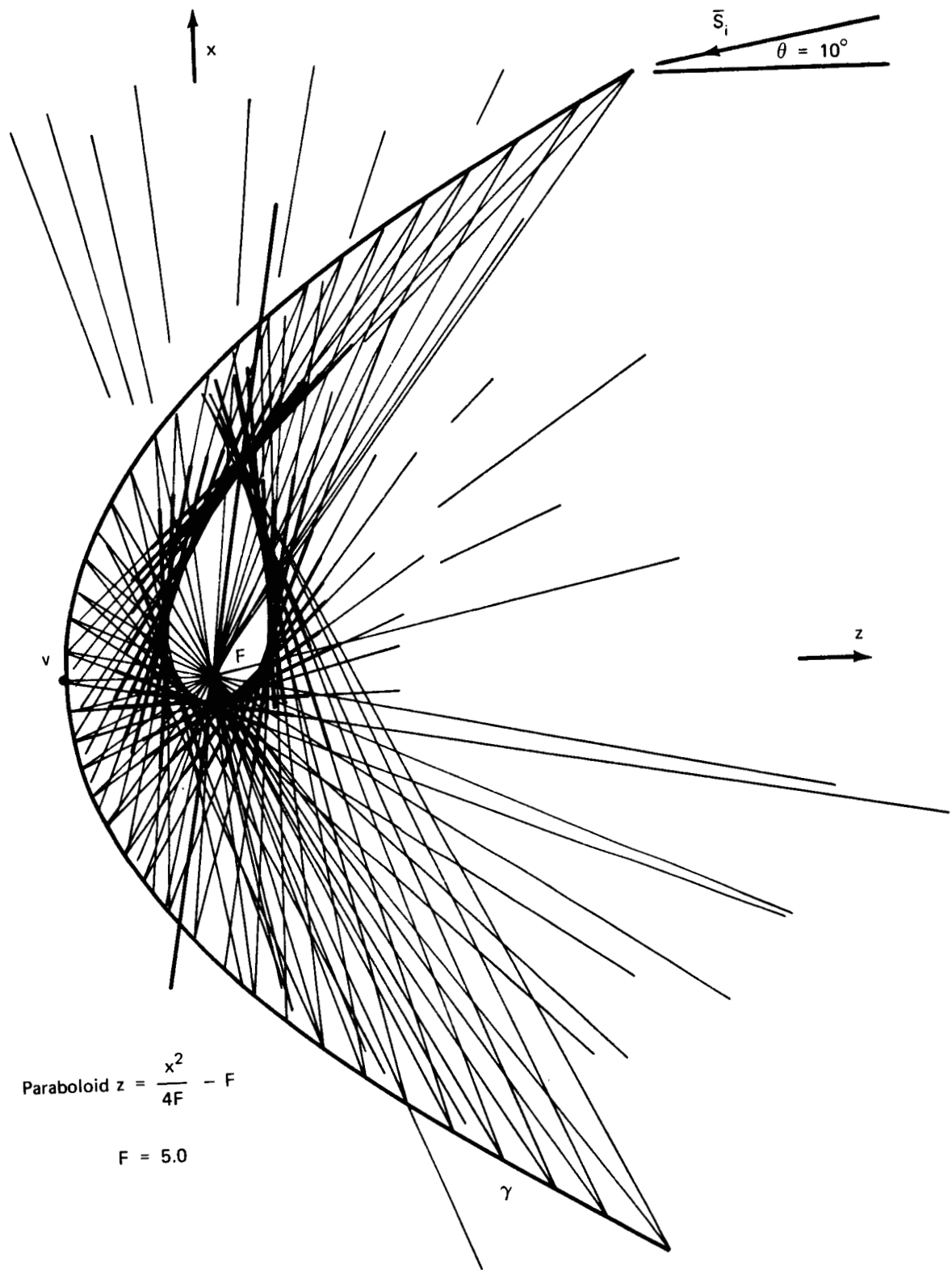


Figure 3. Tschirnhausen's Cubic (caustic arc) for  $\theta_i = 10^\circ$ .

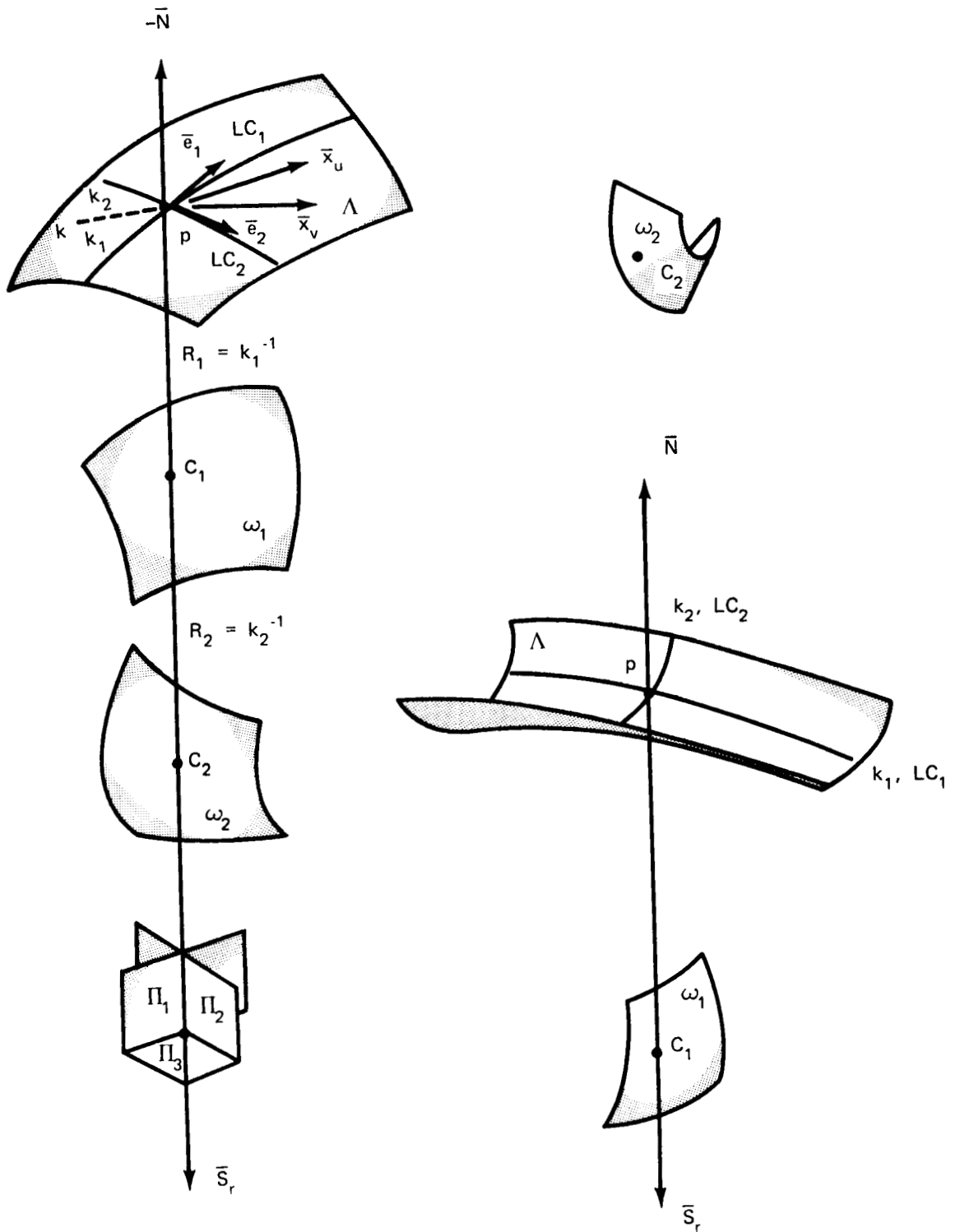


Figure 4. Center Surfaces ( $\omega_1, \omega_2$ ) of a wavefront ( $\Lambda$ ).

## CENTER SURFACES

A review of the theory of center surfaces is useful before setting out to find the surface normals and principal normal curvatures of either wavefronts or reflectors. From the three fundamental equations of differential geometry,

$$I = d\bar{x} \cdot d\bar{x} \quad (3)$$

$$II = -d\bar{x} \cdot d\bar{N} \quad (4)$$

$$III = d\bar{N} \cdot d\bar{N} \quad , \quad (5)$$

the normal curvature is defined as

$$k = \frac{II}{I} = \frac{-d\bar{x} \cdot d\bar{N}}{d\bar{x} \cdot d\bar{x}} = \frac{edu^2 + 2f du dv + gdv^2}{Edu^2 + 2F du dv + Gdv^2} \quad (6)$$

where the surface is:

$$\bar{x} = \bar{x}(u, v) \quad , \quad (7)$$

and the surface normal is

$$\bar{N} = \bar{N}(u, v) \quad (8)$$

Results obtained for principal normal curvature may be verified using Rodriques' formula since it characterizes the eigenvectors.

$$d\bar{N} = -k d\bar{x} \quad . \quad (9)$$

In the preceding,

$$d\bar{x} = \bar{X}_u du + \bar{X}_v dv \quad (10)$$

and

$$d\bar{N} = \bar{N}_u du + \bar{N}_v dv \quad . \quad (11)$$

Here

$$E = \bar{X}_u \cdot \bar{X}_u, F = \bar{X}_u \cdot \bar{X}_v, G = \bar{X}_v \cdot \bar{X}_v \quad (12)$$

and

$$e = L = -(\bar{X}_u \cdot \bar{N}_u) = (\bar{X}_{uu} \bar{X}_u \bar{X}_v) / (EG - F^2)^{1/2} \quad (13)$$

$$f = M = -(\bar{X}_u \cdot \bar{N}_v + \bar{X}_v \cdot \bar{N}_u) = (\bar{X}_{uv} \bar{X}_u \bar{X}_v) / (EG - F^2)^{1/2} \quad (14)$$

$$g = N = -(\bar{X}_v \cdot \bar{N}_v) = (\bar{X}_{vv} \bar{X}_u \bar{X}_v) / (EG - F^2)^{1/2} \quad (15)$$

since

$$\bar{X}_u \cdot \bar{N} = 0, \bar{X}_v \cdot \bar{N} = 0 \quad , \quad (16)$$

and

$$\bar{x}u \cdot \bar{N}v = \bar{X}v \cdot \bar{N}u \quad . \quad (17)$$

The (E, F, G) and (e, f, g) are coefficients of the first and second fundamental forms.

The unit surface normals are obtained from a cross-product of tangents, not necessarily orthogonal, as indicated in Figure 4.

$$\bar{N} = (\bar{X}u \times \bar{X}v) / |\bar{X}u \times \bar{X}v| = (\bar{X}u \times \bar{X}v) / (EG - F^2)^{1/2} \quad (18)$$

Letting

$$\lambda = dv/du \quad , \quad (19)$$

the normal curvature of a surface becomes

$$k = \frac{e + 2f\lambda + g\lambda^2}{E + 2F\lambda + G\lambda^2} \quad . \quad (20)$$

The extrema of k are characterized by

$$dk/d\lambda = 0 \quad , \quad (21)$$

so that

$$k_i = \frac{II}{I} = \frac{f + g\lambda_i}{F + G\lambda_i} = \frac{e + f\lambda_i}{E + F\lambda_i} \quad ; i = 1, 2 \quad (22)$$

See Ref. 5, p. 80; Ref. 21, p. 287.

The  $\lambda_i$  may be found from

$$\lambda_1 + \lambda_2 = -(Eg - Ge)/(Fg - Gf) \quad (23)$$

$$\lambda_1 \lambda_2 = (Ef - Fe)/(Fg - Gf) \quad (24)$$

See Ref. 4, p. 142

The principal directions (eigenvectors) associated with the principal normal curvatures (eigenvalues or characteristic values) are given by

$$\bar{e}_i = (\bar{X}u + \bar{X}v \lambda_i) / H_i \quad , i = 1, 2 \quad (25)$$

where

$$H_i^2 = E + 2F\lambda_i + G\lambda_i^2 \quad , \quad (26)$$

and are always orthogonal since

$$\begin{aligned} \bar{e}_1 \cdot \bar{e}_2 &= (\bar{X}u + \bar{X}v \lambda_1) \cdot (\bar{X}u + \bar{X}v \lambda_2) / H_1 H_2 \\ &= [E + (\lambda_1 + \lambda_2)F + \lambda_1 \lambda_2 G] / H_1 H_2 = 0 \end{aligned} \quad (27)$$

The normal curvature in an arbitrary direction takes the form

$$k = k_1 \cos^2 \alpha + k_2 \sin^2 \alpha \quad , \quad (28)$$

and is known as Euler's theorem.

The derivatives  $\bar{N}_u, \bar{N}_v$  appearing in Rodrigues' formula are given by

$$\bar{N}_u = \frac{fF - eG}{EG - F^2} \bar{X}_u + \frac{eF - fE}{EG - F^2} \bar{X}_v \quad (29)$$

and

$$\bar{N}_v = \frac{gF - fG}{EG - F^2} \bar{X}_u + \frac{fF - gE}{EG - F^2} \bar{X}_v \quad , \quad (30)$$

and are known as the Weingarten equations. Ref. 5, p. 108.

A normal curvature ( $k$ ) is a principal normal curvature ( $k_1, k_2$ ) if and only if  $k$  is a solution of the quadratic

$$(EG - F^2) k^2 - (Eg + Ge - 2Ff) k + (eg - f^2) = 0 \quad (31)$$

Ref. 8, p. 183.

Since the roots of this equation are

$$k_i = \frac{(Eg + Ge - 2Ff) \pm \sqrt{(Eg + Ge - 2Ff)^2 - 4(EG - F^2)(eg - f^2)}}{2(EG - F^2)} \quad , \quad (32)$$

the mean curvature is

$$K_M = \frac{Eg + Ge - 2Ff}{2(EG - F^2)} = \frac{k_1 + k_2}{2} \quad (33)$$

and the Gaussian curvature is

$$K_G = \frac{eg - f^2}{EG - F^2} = k_1 k_2 \quad , \quad (34)$$

so that Equation (28) may be rewritten as

$$k^2 - 2K_M k + K_G = 0 \quad (35)$$

The surface normals along a line of curvature are tangent to two space curves, or edges of regression, at distances  $k_1^{-1}$  and  $k_2^{-1}$  from a point (P) of a given surface. Ref. 5, p. 94; Ref. 21, p. 25. Lines of curvature are always orthogonal. Center surfaces (caustics of two sheets) are the loci of the centers of principal normal curvature of a given surface (wavefront). Figure 4.

The points on a surface are classified as follows:

$$\text{Elliptic:} \quad eg - f^2 > 0 \quad - \quad K_G > 0 \quad (36)$$

$$\text{Hyperbolic:} \quad eg - f^2 < 0 \quad - \quad K_G < 0 \quad (37)$$

Parabolic:	$eg - f^2 = 0$ and $e^2 + f^2 + g^2 \neq 0 \rightarrow$	$K_G = 0$	(38)
Planar:	$e = g = f = 0 \rightarrow$	$K_G = 0$	(39)
Umbilical:	$k = \frac{e}{E} = \frac{f}{F} = \frac{g}{G} =$ constant for all directions		(40)

Ref. 8, p. 177- p. 184; Ref. 16, p. 96; Ref. 6, p. 261

## CAUSTICS FROM DISTORTED WAVEFRONTS

The computational route for obtaining caustics as a set of points from a distorted wavefront is now presented in some detail. A cylindrical net or  $(\sigma, \zeta)$  parametrization is used to describe an idealized spherical wavefront. Aberrations are then introduced along the normal of a Gaussian wavefront and, alternatively, parallel to the system axis when appropriate to achieve simplification of the expressions. Since caustic information is to be obtained as a set of points belonging to center surfaces, machine computations are anticipated at an early stage. The partial derivatives  $\bar{X}_u, \bar{X}_v, \bar{X}_{uu}, \bar{X}_{uv}, \bar{X}_{vv}$  are lengthy, but usually manageable algebraic forms. Forming E, F, G analytically involves vector dot-products. Forming e, f, g involves both vector dot- and cross-products. The latter are not developed analytically.

A physical picture associating reflector, wavefronts, and caustic ( $\omega_1$ ) is given as Figure 5. The wavefronts ( $\Lambda_i$ ) correspond to reception of a 10-degree plane wave by a paraboloidal reflector, and are illustrated in two dimensions only. Caustic analysis will, however, be in three dimensions throughout this document. Figures 2 and 3 are closely related to Figure 5. The cusps of the wavefronts appear to lie on the caustic; this observation is not explored here. Direct determination of the center surfaces or caustics of wavefronts such as  $\Lambda_1, \Lambda_2, \Lambda_3$  is sought for a large class of problems. Figure 5 represents a specific choice of source and surface and is included here for illustrative purposes only.

Introduction of the Gauss/Seidel aberrations of degree 2/4, to the exclusion of the Schwarzschild aberrations of degree 6 and other aberrations, is arbitrary. The method of center surface determination is not restricted to these classic aberrations; they simply provide a useful set of examples encountered in optics and microwaves. The Gaussian sphere may be associated with the class of problems that regards circular apertures. It is replaced, for other geometries, by conformable reference wavefronts. Cylindrical and toroidal geometries are examples where the Gaussian sphere is inappropriate. Ref. 17, Ref. 18.

Appendix A and Appendix B contain the details pertaining to distorted wavefronts for the Gauss/Seidel aberrations when perturbations are directed parallel to the system axis (Z) or along the normal ( $\bar{N}_s$ ) to the Gaussian sphere, respectively. The latter case is illustrated in Figure 6. It can be seen that the set of normals for  $\zeta$  equals a constant on the Gaussian sphere is coplanar. This is not necessarily true for the corresponding set of normals on the distorted wavefront. As a result, a planar arc on the Gaussian sphere maps to a pair of three dimensional space curves or edges of regression lying on the caustic surface branches ( $\omega_1, \omega_2$ ). A caustic surface may be represented by a sufficiently large number of such curves ( $\Gamma$ ) in  $(x, y, z)$  space. A single curve may be dealt with by considering projections onto the plane  $\zeta$  equals a constant and a plane orthogonal to it by forming

$$R_{1,2} \cdot {}_1\bar{N}_\Lambda \cdot \hat{k} = R_{1,2} \cdot {}_1\bar{N}_\Lambda \cdot (0, 0, 1) \quad , \quad (41)$$

$$R_{1,2} \cdot {}_1\bar{N}_\Lambda \cdot {}_1\bar{N}_\parallel = R_{1,2} \cdot {}_1\bar{N}_\Lambda \cdot (-\sin \zeta, \cos \zeta, 0) \quad , \quad (42)$$

$$R_{1,2} \cdot {}_1\bar{N}_\Lambda \cdot {}_1\bar{N}_\perp = R_{1,2} \cdot {}_1\bar{N}_\Lambda \cdot (\cos \zeta, \sin \zeta, 0) \quad , \quad (43)$$

where  ${}_1\bar{N}_\Lambda, {}_1\bar{N}_\parallel, {}_1\bar{N}_\perp$ , are unit normals to the distorted wavefront ( $\Lambda$ ) and the projection planes, respectively. Here  $R_{1,2}$  are the principal normal radii of curvature.

Three dimensional isometric representation of the caustic surface branches ( $\omega_1, \omega_2$ ) is to be preferred to the projection described above.

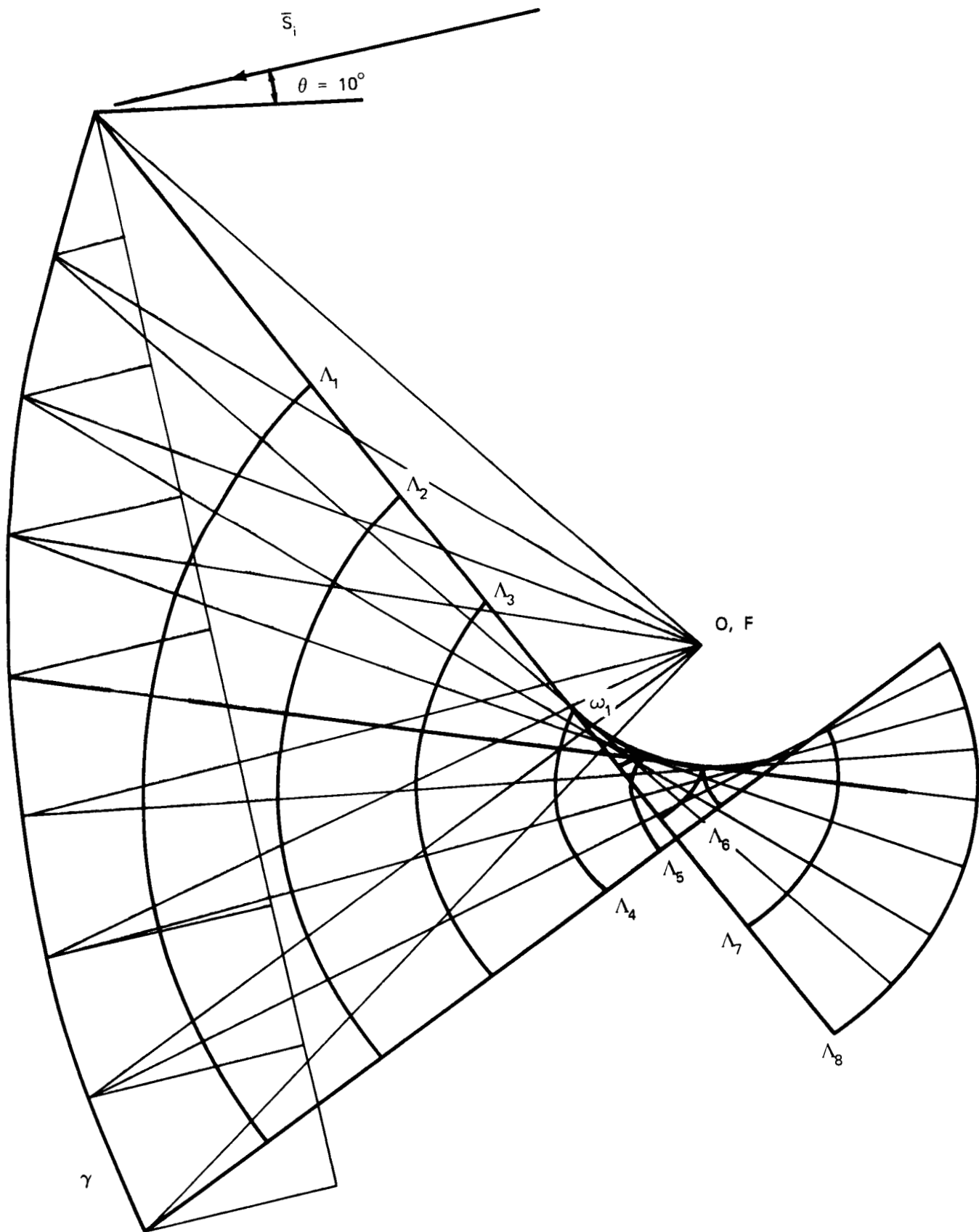


Figure 5. Reflector ( $\gamma$ ), Wavefronts ( $\Lambda_i$ ), and Caustic ( $\omega_1$ ).

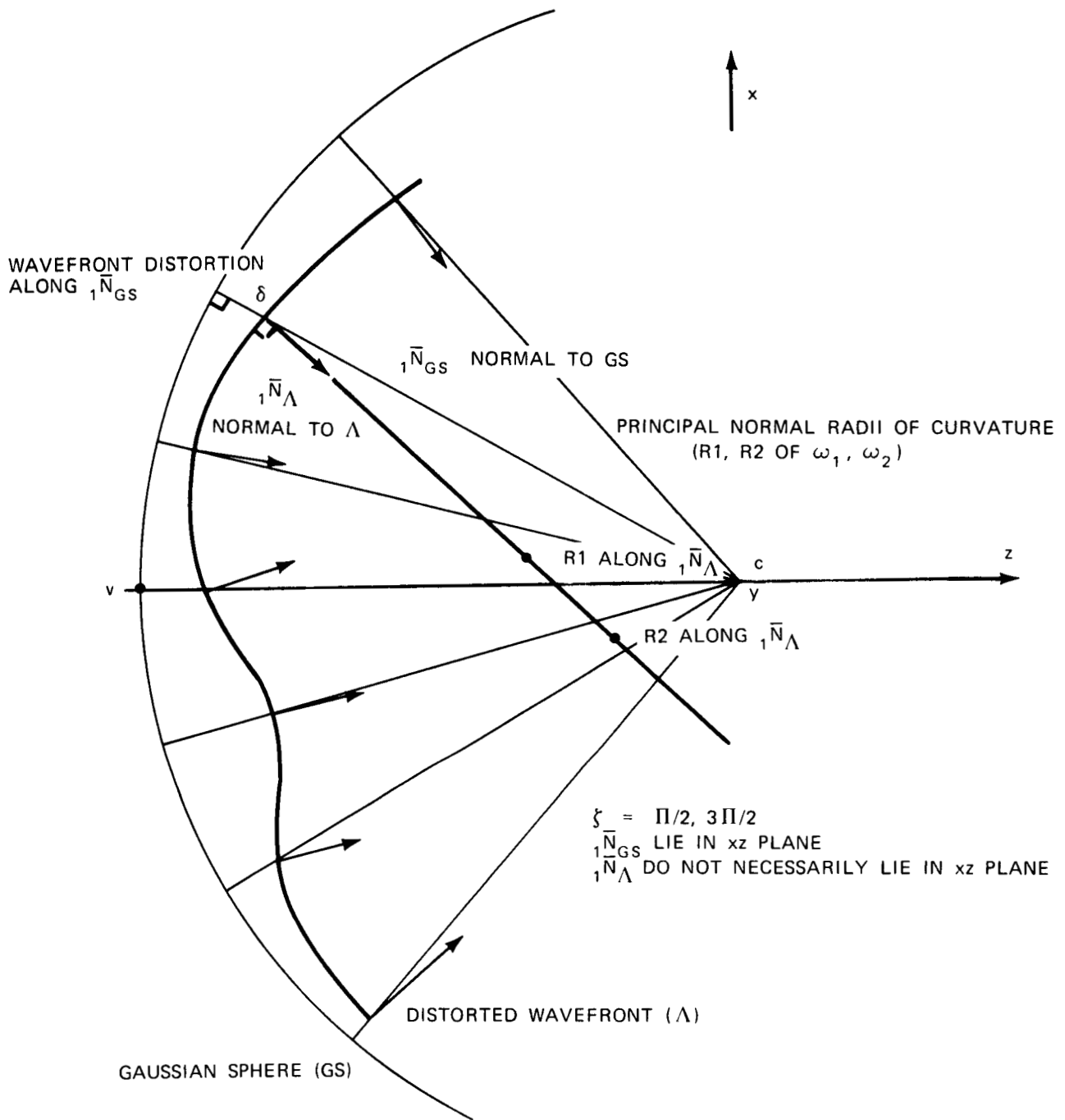


Figure 6. Mapping of Surfaces GS:  $\Lambda: \Omega(\omega_1, \omega_2)$ .

## CAUSTICS FROM FLUX DENSITY SINGULARITIES

Caustic surfaces may be obtained from an algorithm that permits the computation of flux density at generic field points with the exception of the caustic coordinates. Refs. 11, 12, 13. Information regarding the caustics is obtained by exploiting a singularity of the flux-density formulation

$$F_{ds_1-ds_2} = \frac{C_{R,T} I \cos \varphi_i \cos \psi_i}{|a_0 + a_1 r_2^2 + a_2 r_2^4|} \quad (44)$$

The denominator of equation (44) is set equal to zero, and the resulting quadratic is solved for distances  $R_{21}$ ,  $R_{22}$  along a reflected ray. Wavefronts do not enter explicitly, and caustics are obtained under this approach in terms of the intrinsic Gaussian, mean, and normal curvatures ( $K_G$ ,  $K_M$ ,  $K_N$ ) of a deflector surface and a specified source of illumination.  $K_N$  is determined by the intersection of the plane formed by the deflector normal and the incident ray with the deflector surface.

In the preceding equation  $C_{R,T}$  is a reflection or transmission coefficient associated with a deflector,  $I$  is the irradiance due to a source,  $\varphi_i$  and  $\psi_i$  are angles of incidence on the deflector and receiver, respectively. For the present discussion, reflectors only,

$$C_{R,T} = C_R = 1.0 \quad (45)$$

The coefficients  $a_0$ ,  $a_1$ ,  $a_2$  for reflection are

$$a_0 = \cos \varphi_i \quad (46)$$

$$a_1 = -2(2K_M \cos^2 \varphi_i + K_N \sin^2 \varphi_i) + 2 \cos \varphi_i / (r_1) \quad (47)$$

$$a_2 = 4K_G \cos \varphi_i - 2(2K_M \cos^2 \varphi_i + K_N \sin^2 \varphi_i) / (r_1) + \cos \varphi_i / (r_1)^2 \quad (48)$$

Several specializations are made for the discussion that follows. Incidence on a planar receiver (film) is not anticipated, therefore the factor  $\cos \psi_i$  is set to unity to obtain the flux-density field. Reflection is assumed to be perfect and irradiance is arbitrarily taken to be unity also. For illumination by a plane wave, the distance ( $r_1$ ) from source to reflector is unbounded so that the following simplification is achieved:

$$F_{ds_1-ds_2} = \frac{\cos \varphi_i}{|\cos \varphi_i - 2(2K_M \cos^2 \varphi_i + K_N \sin^2 \varphi_i) r_2 + 4(K_G \cos \varphi_i) r_2^2|} \quad (49)$$

$$r_2 = R_{21}, R_{22} = \frac{(2K_M \cos^2 \varphi_i + K_N \sin^2 \varphi_i) \pm \sqrt{(2K_M \cos^2 \varphi_i + K_N \sin^2 \varphi_i)^2 - 4K_G \cos^2 \varphi_i}}{4K_G \cos \varphi_i} \quad (50)$$

The utility of the flux-density method may be demonstrated by several examples. Consider the paraboloid and, following the sign conventions of Ref. 11, take the principal normal curvatures of the reflector surface to be

$$k_1 = \frac{-4F^2}{(4F^2 + \sigma^2)^{3/2}}, \quad (51)$$

and

$$k_2 = \frac{-1}{(4F^2 + \sigma^2)^{1/2}}, \quad (52)$$

using standard procedures of differential geometry. Ref. 17, Ref. 5.

When a plane-wave is axially directed upon a paraboloid rotational symmetry exists and

$$K_N = k_1 \quad (53)$$

for every planar cut containing the system axis. From this

$$K_M = \frac{-1}{2} \frac{(8F^2 + \sigma^2)}{(4F^2 + \sigma^2)^{3/2}} = \frac{k_1 + k_2}{2} \quad , \quad (54)$$

and

$$K_G = \frac{4F^2}{(4F^2 + \sigma^2)^2} = k_1 k_2 \quad . \quad (55)$$

It can be shown that

$$\cos^2 \varphi_1 = \frac{4F^2}{4F^2 + \sigma^2} \quad (56)$$

and

$$\sin^2 \varphi_1 = \frac{\sigma^2}{4F^2 + \sigma^2} \quad (57)$$

so that the radical of equation (50) vanishes. The roots of  $r_2$  are then equal.

$$|r_2| = |R_{21}| = |R_{22}| = \frac{(4F^2 + \sigma^2)}{4F} \quad (58)$$

Recalling the equations of a parabola

$$z = \frac{\sigma^2}{4F} - F \quad , \quad (59)$$

$$\rho = 2F / (1 + \cos 2 \varphi_1) \quad , \quad (60)$$

and

$$\cos 2 \varphi_1 = \frac{|z|}{(\sigma^2 + z^2)^{1/2}} \quad , \quad (61)$$

the result

$$\rho = |r_2| \quad (62)$$

can be shown. The interpretation is that all  $|r_2|$ , directed along a reflected ray, terminate on the focal point of the paraboloid. That is, the caustic surfaces  $\omega_1$  and  $\omega_2$  degenerate to point caustics that are congruent with the focus (F), in the present analysis, for an axially-directed plane-wave source. See Ref. 6, p. 259.

When the incident plane wave is not axially directed, equation (50) is evaluated. For every value ( $\sigma$ ) of the radial net the local incidence angle ( $\varphi_i$ ) at  $\gamma$  may be found using

$$\begin{aligned} ({}_1\bar{N}\gamma) \cdot (-{}_1\bar{S}_i) &= {}_1\bar{N}\gamma \cdot \bar{S}_i = \cos \varphi_i \\ \text{(concave side)} &\quad \text{(convex side)} \end{aligned} \quad (63)$$

where both  ${}_1\bar{N}\gamma$  and  ${}_1\bar{S}_i$  are unit vectors.

An xz-plane cut through the caustic surfaces  $\omega_1, \omega_2$  for a 10-degree plane wave source is shown in Figure 7. Tschirnhausen's cubic ( $\omega_1$ ) is recovered directly, without any representation of the received wavefront as a set of points along the reflected rays ( $\bar{S}_r$ ). A second caustic branch ( $\omega_2$ ) is also obtained here, and Figure 7 should be compared with Figure 3. The set of reflected rays in the xz plane of Figure 3 did not provide any information about caustic branch ( $\omega_2$ ); the three dimensional representation is required.

Figure 7, for the paraboloid, may be obtained by plotting  $R_{21} {}_1\bar{S}_r$  and  $R_{22} {}_1\bar{S}_r$  from reflector ( $\gamma$ ) to caustic sheets ( $\omega_1, \omega_2$ ). The  $R_{21}, R_{22}$  are effectively eigenvalues of latent wavefronts which intersect ( $\gamma$ ) at every ( $\sigma, \zeta$ ) pair. See Figure 5. A more expedient approach is to plot vectors

$$\bar{x}(\omega_1) = \bar{x}(P) - (R_{21}) {}_1\bar{S}_r \quad (64)$$

and

$$\bar{x}(\omega_2) = \bar{x}(P) - (R_{22}) {}_1\bar{S}_r \quad (65)$$

from the origin (0). Similarly, the coordinates of a computed flux-density (FD) may be written as

$$\bar{x}(\text{FD}) = \bar{x}(P) - (R_2) {}_1\bar{S}_r \quad (66)$$

If  $R_2$  is adequately subdivided ( $\Delta R_2$  small), the contour mapping problem of the authors Burkhard and Shealy may be relieved by forming a "look-up table" for each ray ( ${}_1\bar{S}_r$ ) so that preselected values may be located directly. This obviates the need for interpolation estimates minimizes errors, and is readily adapted to automatic plotting methods providing computation time is not excessive.

Figure 8 shows the overall flux-density picture with condensing and diverging pseudo-spherical waves. The departure from a Gaussian sphere is dominated by a linear phase gradient of weight ( $\omega_{1,1}$ ) and a comatic aberration gradient of weight ( $\omega_{1,3,1}$ ) as described in Appendix B of this document. In the flux-density approach the distorted wavefront per se is never identified.

Figure 9 shows the flux-density picture in the vicinity of the caustic surfaces ( $\omega_1, \omega_2$ ) as seen in the (x, z) plane. It is particularly important to identify the ray bundle associated with the flux-density mapping and the intercepts of the bounding rays of that bundle with the caustic curves. Within the ray bundle there is a region where flux-density values superimpose. The introduction of rays outside of the bundle ( $\bar{S}_r', \bar{S}_r''$ ) enlarges that region. See Ref. 6, p. 259; p. 262.

When an axial plane wave illuminates a portion of a sphere the results are not as degenerate as for the paraboloid. A pseudo-focus appears at  $(0,0, -c/2)$ , a line caustic ( $\omega_2$ ) forms, and a surface caustic ( $\omega_2$ ) may be associated with a nephroid generating arc rotated about the reflector (z) axis. Figure 10. With paraxial reception, the primary difference is a rotation and translation of the caustic surfaces with some distortion (Figure 11). It is often instructive to trace the progression of the points  $\bar{x}(\omega_1), \bar{x}(\omega_2)$  as radial variable ( $\sigma$ ) is updated for some azimuthal value ( $\zeta$ ) on the reflector ( $\gamma$ ). A mapping of the flux-density for the sphere with inclined incident plane wave is given as Figure 12. Condensing and diverging waves are seen here also, but the fine-structure in the vicinity of the displaced pseudo-focus differs greatly from the previous paraboloid example.

Although this document is primarily concerned with identifying the means for obtaining caustic/flux density information, and verifying some of the formulation, the practical implications for microwaves and optics are also of interest. The paraboloidal and spherical reflector examples were selected because of the wide application of these surfaces as focussing or collecting devices. Caustic analysis appears to offer an economical means for obtaining high-frequency focal region information in three-dimensional space. The analytical generation of coordinates for two caustic sheets, with varying degrees of degeneracy, provides insight not readily obtained by the tangent approach found in many textbooks and journal articles. Annexation of flux-density greatly enhances the value of the classic caustic analysis of wavefronts. Extensions to edge-diffraction, including various approaches such as the geometrical

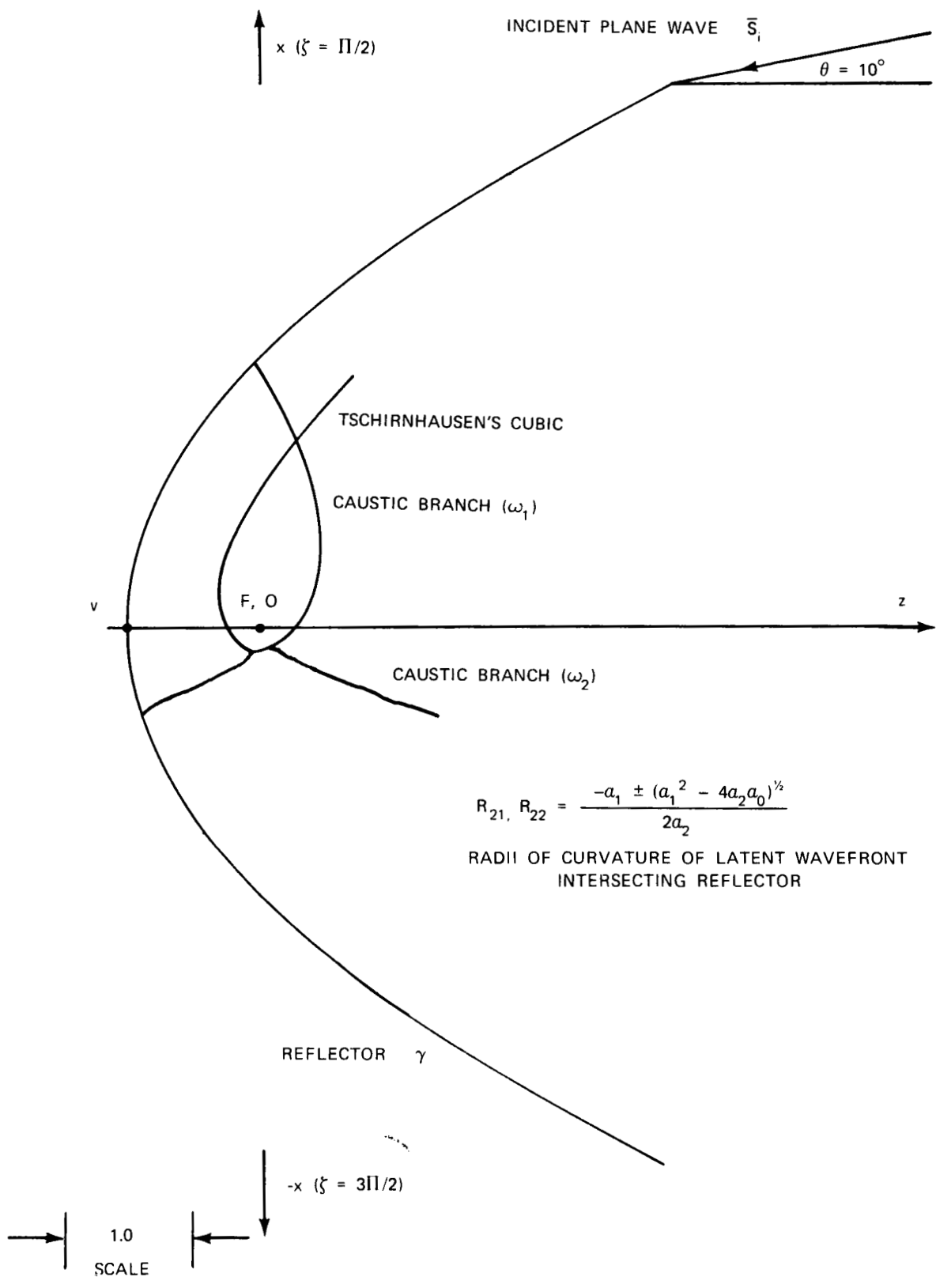


Figure 7. Caustic Surfaces from Flux-Density Singularities (Paraboloid  $F = 1.0$ )

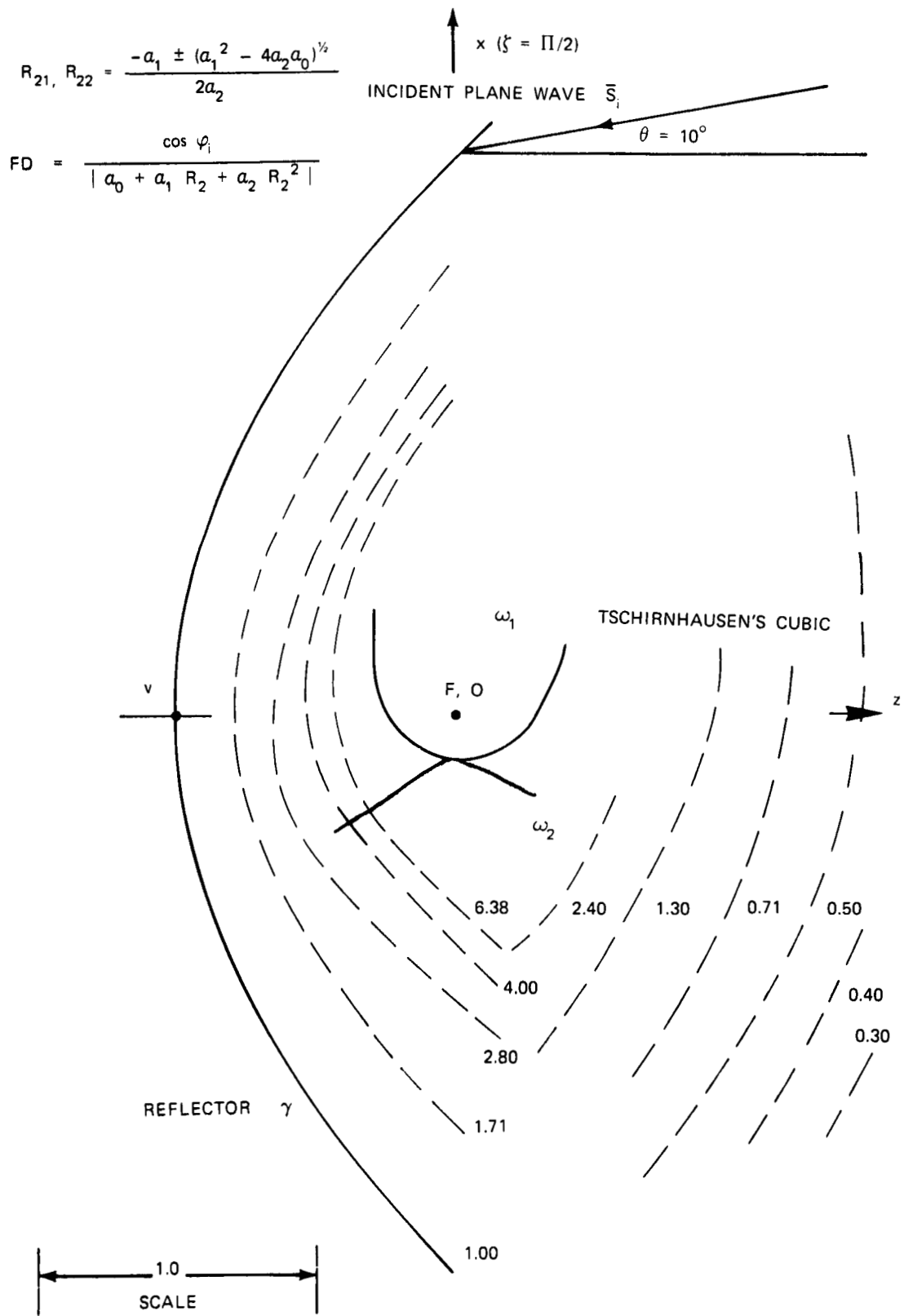


Figure 8. Caustic Surfaces and Flux-Density (Paraboloid  $F = 1.0$ )

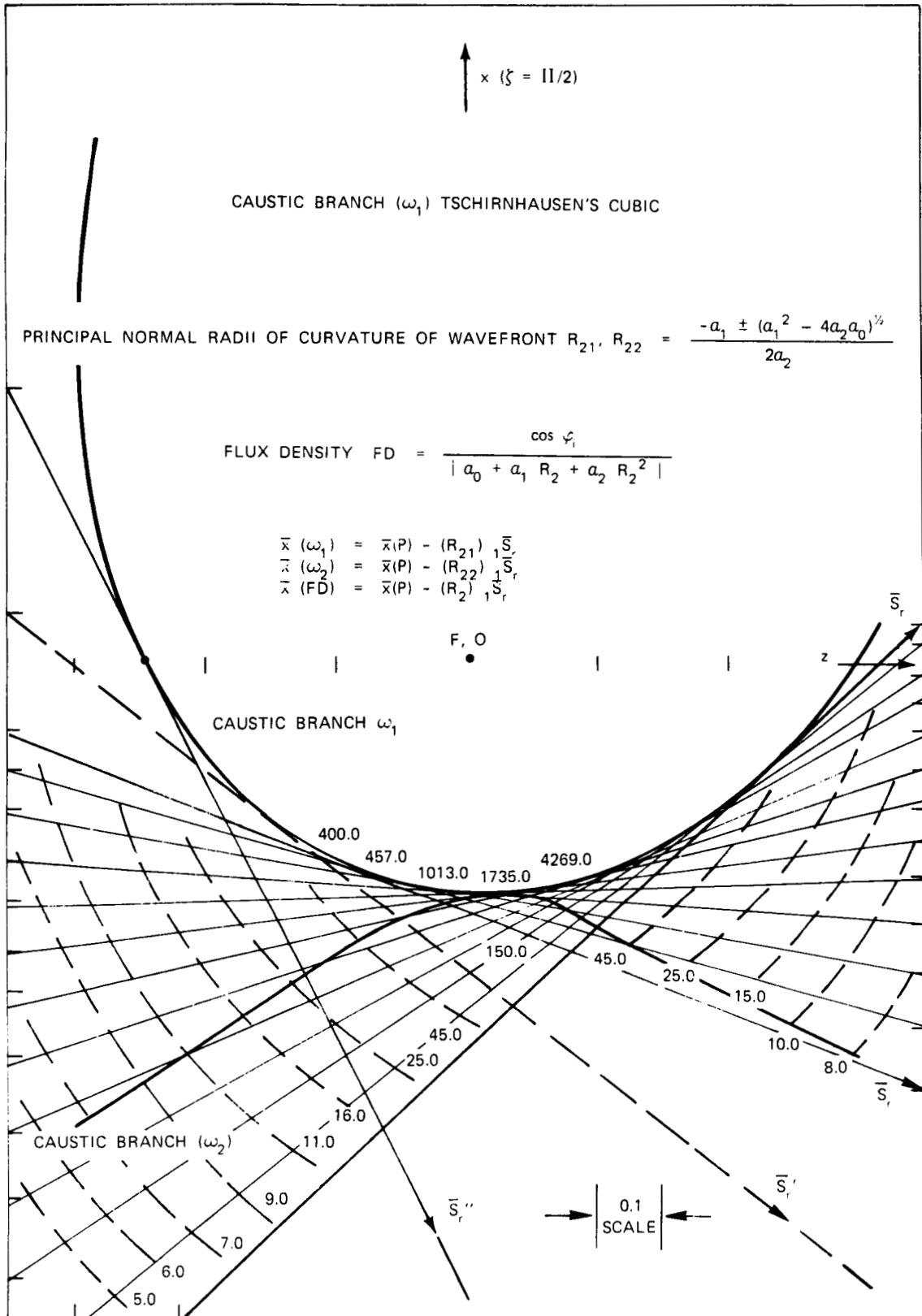


Figure 9. Caustic Surfaces and Flux-Density (Paraboloid  $F = 1.0$ )

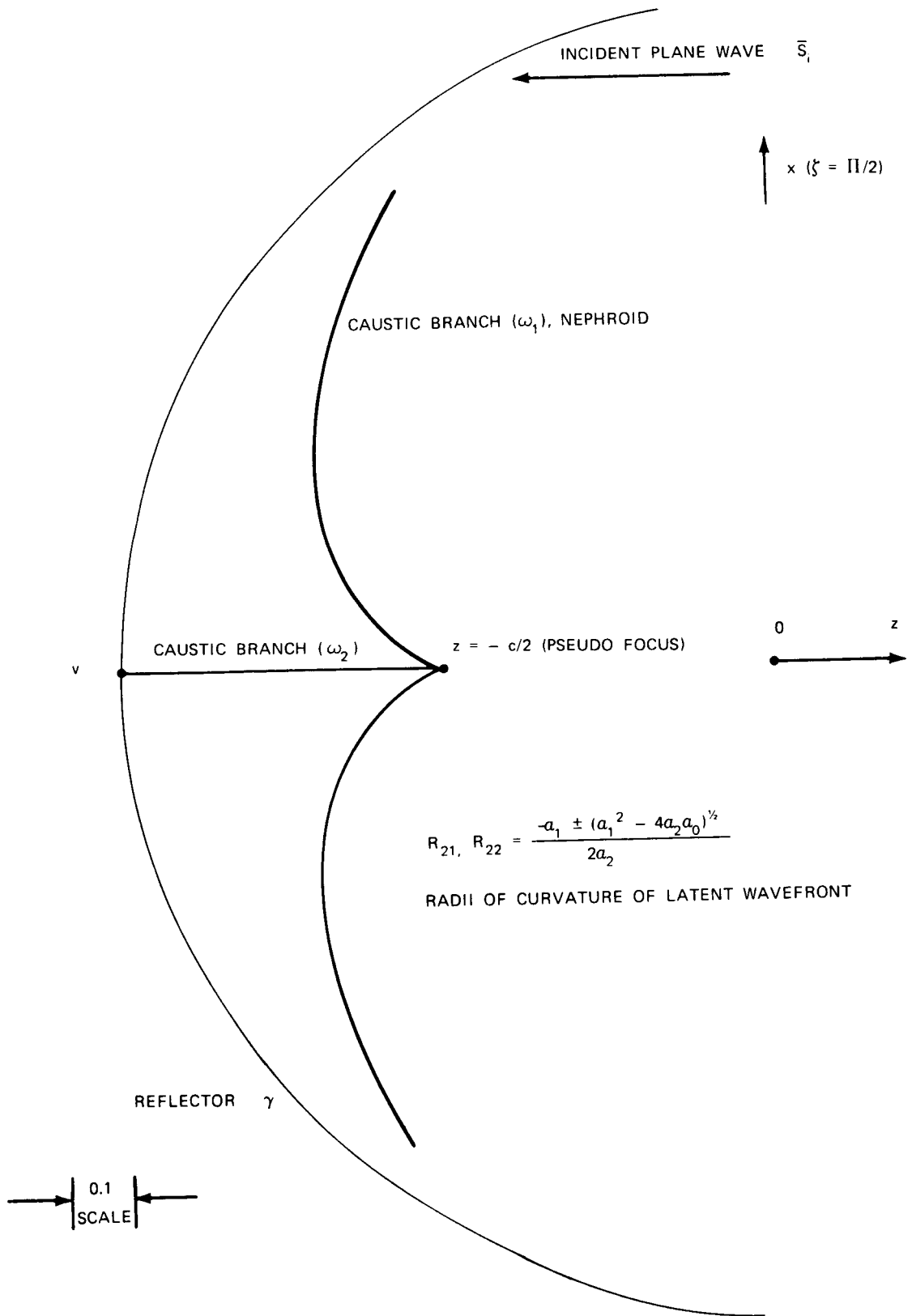


Figure 10. Caustic Surfaces from Flux-Density Singularities (Sphere  $C = 1.0$ )

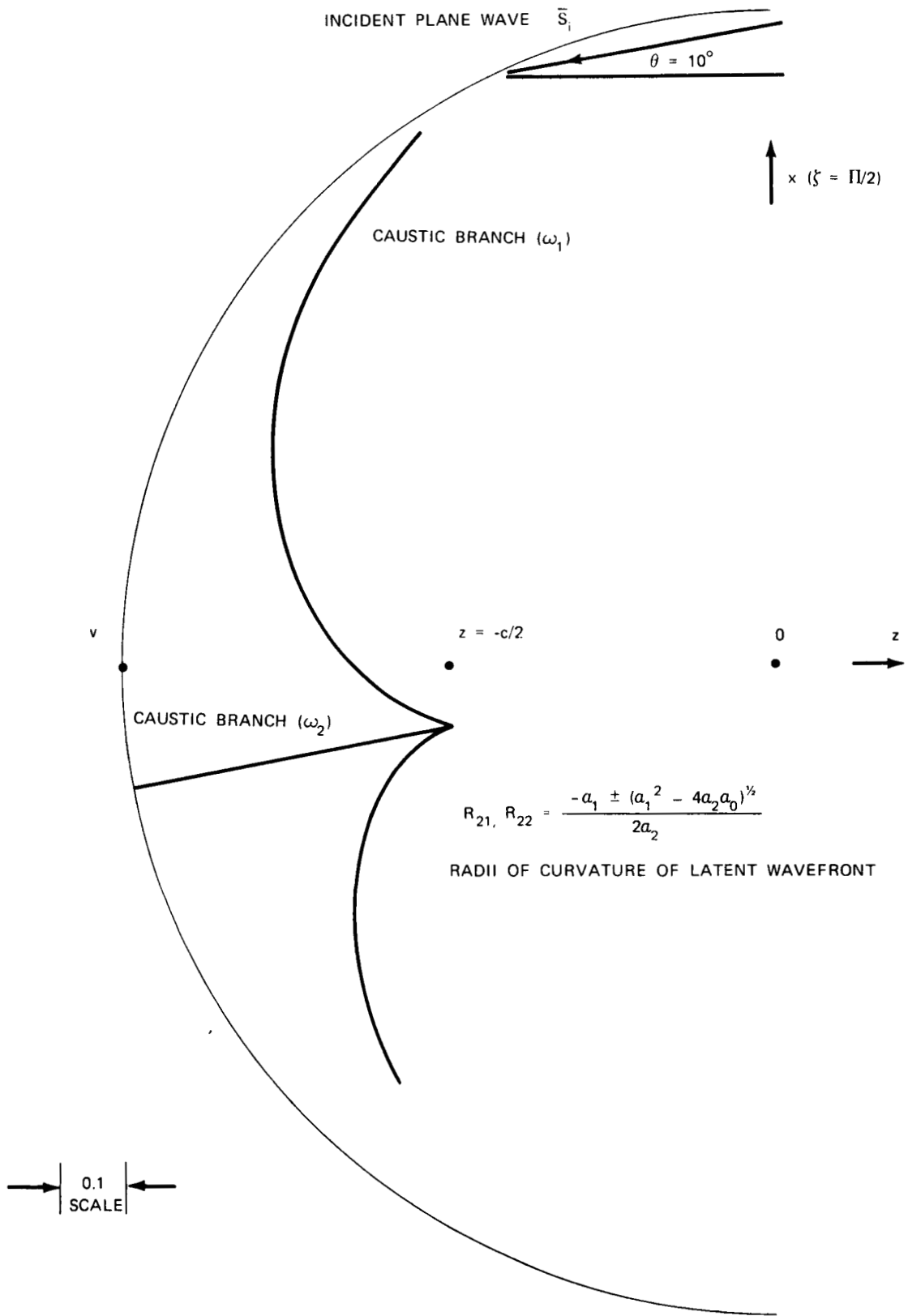


Figure 11. Caustic Surfaces From Flux-Density Singularities (Sphere  $C = 1.0$ )

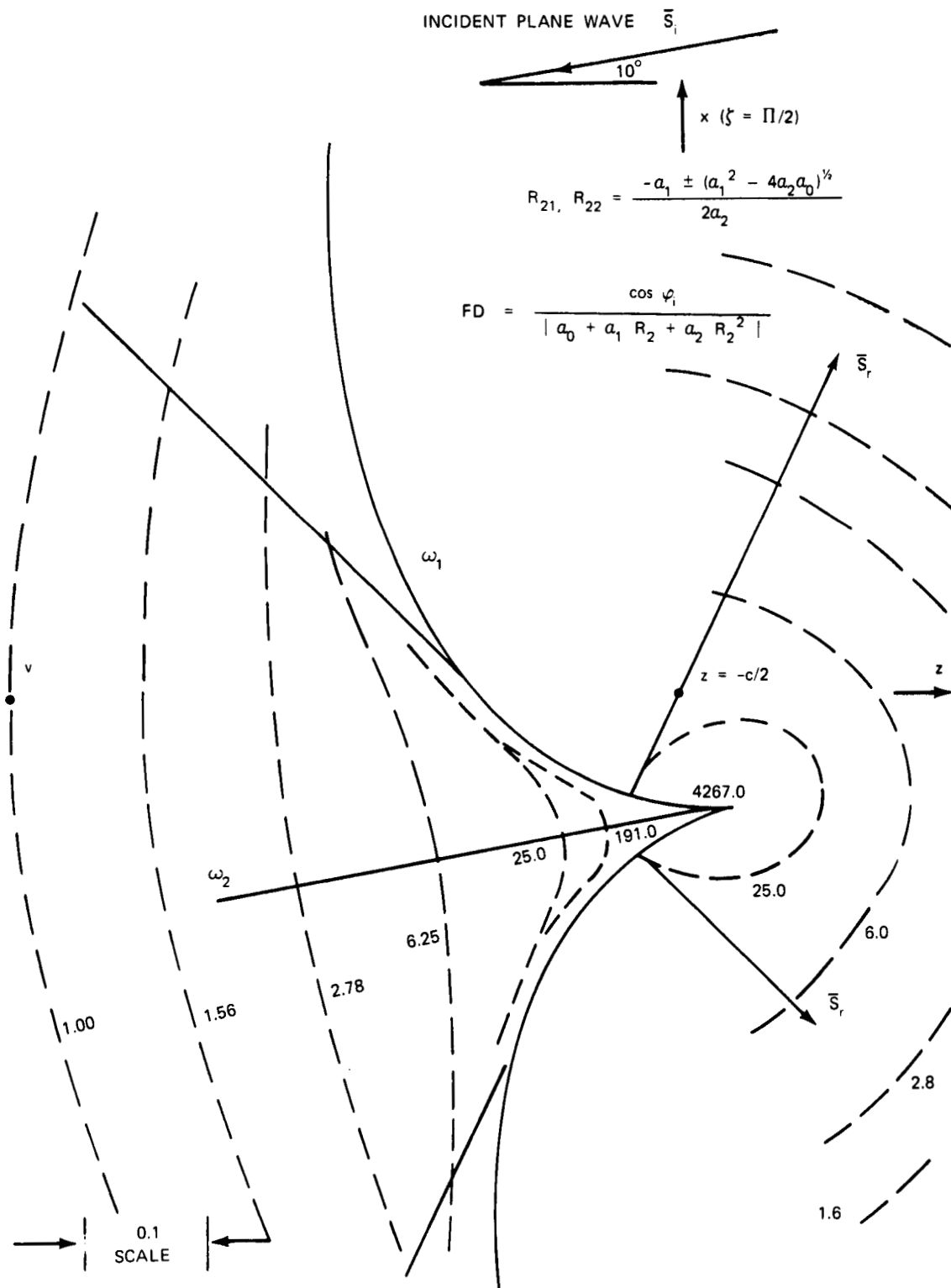


Figure 12. Caustic Surfaces and Flux Density (Sphere C = 1.0)

theory of diffraction (GTD) and the uniform asymptotic theory of diffraction (UTD), lie beyond the scope of the present discussion. Ref. 24, pp. 67-119. Also, the caustic approach is not placed in competition with other means for obtaining focal-region information (i.e. physical optics for example). An example of such a comparison may be found in Ref. 25, p. 477. Also see Ref. 30, p. 266 for the fine structure of a cusp caustic and Ref. 6, p. 263 for examples of smooth and cusp caustics.

The interested reader may wish to review the design of a line-feed built by the Cornell University Center for Radiophysics and Space Research for the 1000-foot spherical reflector of the Arecibo Ionospheric Observatory in Puerto Rico. Refs. 22, 26, 27, 28. Additional information on a line-source corrector for a large spherical reflector is found in Ref. 29. It is noted that every point of the nephroid ( $\omega_1$ ) in Figure 10 is the result of the intersection of two rays, and that every point of the line caustic ( $\omega_2$ ) is the result of the intersection of a cone of rays. Ref. 23, p. 118. The implications of the number of ray intersections at various points in the focal region (cusp of a caustic) with respect to field values is discussed in Ref. 31, pp. 1331-1358. Details pertaining to the electromagnetic diffraction in the focal region of a spherical mirror under oblique illumination may be found in Refs. 32, 33, and 34.

## CAUSTICS FROM A TENSOR ALGORITHM

A method of obtaining the equations of caustics by means of a "tensor" algorithm has been found in the literature. Ref. 19. The cited source does not contain the derivation of the method. It asserts that

$$\bar{x}_i = x_i + \frac{pX_i}{(\gamma - \Omega)} \quad , \quad (67)$$

vectorially. Here  $p$  is a scalar,  $X_i$  is a unit vector along a reflected ray,  $x_i$  is a vector to the reflector  $\gamma$ , and  $\bar{x}_i$  is a vector to the caustic ( $\Omega$ ) of two sheets or branches ( $\omega_1, \omega_2$ ) as illustrated in Figure 13.

The central problem is to find, explicitly, an equation giving the distance ( $p$ ) to a caustic ( $\Omega$ ) that is known in terms of a family of tangent rays ( $\bar{S}_i$ ) from a reflector ( $\gamma$ ). An equation is given in Ref. 19 for the unknown distance

$$p = \frac{-g_{1\alpha} du_\alpha}{G_{1\alpha} du_\alpha} = \frac{-g_{2\alpha} du_\alpha}{G_{2\alpha} du_\alpha} \quad , \quad (\alpha = 1, 2) \quad , \quad (68)$$

together with tensors

$$G_{\alpha\beta} = \frac{\partial X_i}{\partial u_\alpha} \frac{\partial X_i}{\partial u_\beta} \quad ; \quad (\alpha, \beta = 1, 2) \quad , \quad (69)$$

and

$$g_{\alpha\beta} = \frac{\partial x_i}{\partial u_\alpha} \frac{\partial x_i}{\partial u_\beta} \quad ; \quad (\alpha, \beta = 1, 2) \quad . \quad (70)$$

In Ref. 19, for the paraboloidal reflector,

$$u_1 = \rho, u_2 = \theta \quad (71)$$

are radial and azimuthal variables of an orthogonal (cylindrical) net, and an inclined plane wave is assumed to be the source of rays ( $\bar{S}_i$ ).

The reason for introducing the second-rank tensors  $g_{\alpha\beta}$  and  $G_{\alpha\beta}$  is obscure, and may have been merely a desire for a compact expression for distance ( $p$ ), but this is speculation. A derivation of the present method of obtaining the equation of a caustic surface directly from a specification of the source and the reflector, without introducing the notion of flux-density, is given below. Beginning with equation (67),

$$d\bar{x}_i = dx_i + d(pX_i) \quad . \quad (72)$$

Since  $X_i$  is a unit vector,

$$X_i \cdot dX_i = 0 = d\bar{x}_i \cdot dX_i \quad , \quad (73)$$

and

$$\left[ \left( \frac{\partial x_i}{\partial u_\alpha} \right) du_\alpha + \left( p \frac{\partial X_i}{\partial u_\alpha} \right) du_\alpha + (X_i) \frac{dp}{du_\alpha} \right] \cdot \left( \frac{\partial X_i}{\partial u_\alpha} \right) du_\alpha = 0 \quad (\alpha = 1, 2) \quad (74)$$

From this,

$$\left[ \frac{\partial x_i}{\partial u_1} \frac{du_1}{du_2} + p \frac{\partial X_i}{\partial u_1} \frac{du_1}{du_2} + \frac{\partial x_i}{\partial u_2} + p \frac{\partial X_i}{\partial u_2} \right] \cdot \left[ \frac{\partial X_i}{\partial u_1} \frac{du_1}{du_2} + \frac{\partial X_i}{\partial u_2} \right] = 0 \quad (75)$$

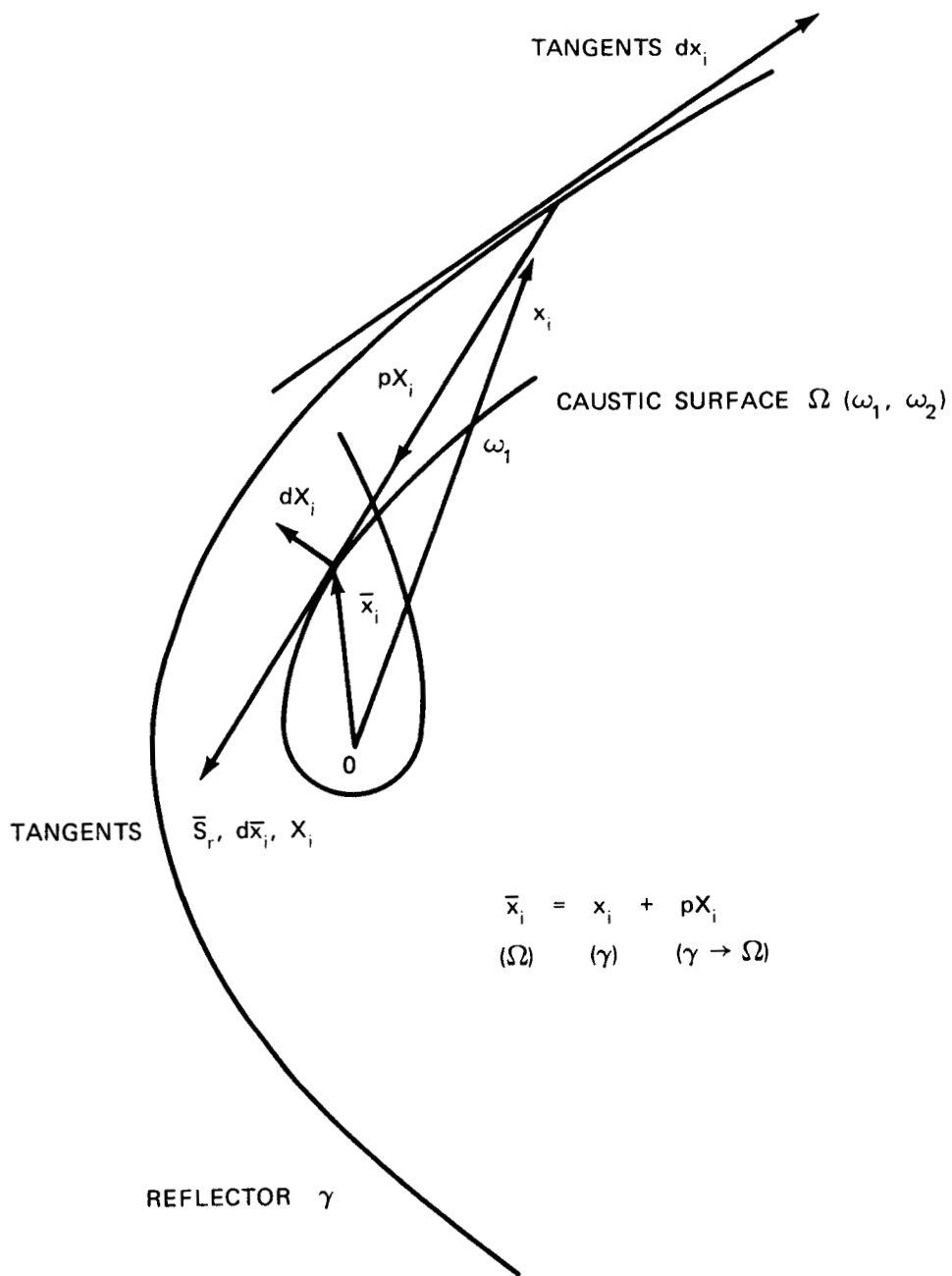


Figure 13. Caustic Surfaces from a Tensor Algorithm.

In compact notation,

$$(g_{11} + p G_{11}) \left( \frac{du_1}{du_2} \right)^2 + (g_{21} + p G_{21} + g_{12} + p G_{12}) \left( \frac{du_1}{du_2} \right) + (g_{22} + p G_{22}) = 0 \quad (76)$$

If the ratio ( $du_1/du_2$ ) is to have only one value,

$$(g_{21} + p G_{21} + g_{12} + p G_{12})^2 - 4 (g_{11} + p G_{11}) (g_{22} + p G_{22}) = 0. \quad (77)$$

For the paraboloid with off-axis plane-wave,

$$G_{12} = G_{21} \quad (78)$$

and

$$g_{12} = g_{21} = 0 \quad (79)$$

The last equation is attributed to the existence of a normal rectilinear congruence in Ref. 19, but appears to be due to the selection of an orthogonal ( $\rho, \theta$ ) net.

Applying both equations, (78) and (79), the simplification obtained for this specialization is

$$p^2 (G_{12})^2 - (g_{11} + p G_{11}) (g_{22} + p G_{22}) = 0 \quad (80)$$

and a quadratic in ( $p$ ) is recovered:

$$p^2 + \frac{(g_{22} G_{11} + g_{11} G_{22}) p}{(G_{11} G_{22} - G_{12}^2)} + \frac{g_{11} g_{22}}{(G_{11} G_{22} - G_{12}^2)} = 0 \quad (81)$$

The roots of the preceding quadratic,

$$p = p_1, p_2 \quad (82)$$

are not radii of curvature, but they stretch or compress the unit vector  $X_i$  (or  $\bar{S}_i$ ) to locate points of the caustic branches ( $\omega_1, \omega_2$ ). In this respect ( $p$ ) is operationally identical to ( $R_2$ ), associated with the flux-density singularity and discussed previously. The derivation, above, circumvents an assumption of Ref. 19 that there exists a  $du_1$  and, independently, a  $du_2$  such that utilization of equation (75) yields the equal lengths ( $p$ ). Introducing the ratio ( $du_1/du_2$ ) results in the same quadratic in ( $p$ ) obtained in Ref. 19, but admits a simultaneous pair  $du_1, du_2$  and avoids "eliminating" these factors in a separate operation.

A specific result that utilizes the preceding method is given in Appendix C of this document. The equation for the caustic surfaces is obtained for a paraboloid illuminated by an off-axis plane wave.

## CONCLUSION

The present document has discussed several methods for determining analytical caustic surfaces. It was shown that the mapping of focal regions is an extended study of surfaces including the source or incident wavefront, the reflector, and the reflected wavefront in addition to the caustic surfaces, themselves. A review of the classical three-dimensional treatment of center surfaces, as applied to distorted wavefronts, was augmented by the flux-density analysis. The latter, predicated on the Jacobian of a mapping, obtained the caustic surfaces directly from a specification of the illuminating function and the reflector, to the exclusion of an identifiable physical wavefront. Only the intrinsic Gaussian, mean, and normal curvature, associated with the incident ray, were required to obtain both caustic branches by exploiting a singularity of the flux-density equation.

This effort progressed until it became apparent that a second document would be needed to display isometric views of the caustic surfaces. The computational aspects of the problem have been dealt with using the TURBO PASCAL language, but a need for automatic plotting capability with a "hidden-line" feature seemed essential to enhance presentation, reduce the amount of labor, and guard against human error. An extension of the wavefront approach to a Gaussian sphere, rather than a hemisphere, is also being implemented. A discussion of multiple reflection, or higher epicycloids, previewed by both the paraboloidal and spherical reflector examples presented here, has been deferred to a second document together with such topics as multiple and extended sources. The latter raises the question of relative phase, and the phase of the caustic surfaces in general. Speculation regarding "intersecting" and "nearly-intersecting" ray density, and other controversial subjects, were also set aside to keep this paper within reasonable bounds.

## **ACKNOWLEDGMENTS**

The author is indebted to R. Meneghini and J. Turkiewicz, Code 675, Laboratory for Oceans, GSFC, for helpful discussions regarding caustic surface analysis and catastrophe theory, and assistance with the IBM personal computer, respectively. The derivation of the so-called tensor algorithm presented in this document is due to Dr. M. Kao of Science Applications Research (SAR). The development of several very useful Turbo Pascal programs for computing flux density and caustic surface coordinates is due to M. McMichen of the General Software Corporation (GSC), who worked under the direction of M. Marrie, Code 653, ADP Laboratory, GSFC.

## REFERENCES

1. Herzberger, M., "Modern Geometrical Optics," Interscience Publishers, Inc., 1958.
2. Theocaris, P. S. and Michopoulos, J. G., "Generalization of the Theory of Far-Field Caustics by the Catastrophe Theory," *Applied Optics*/Vol. 21, No. 6, 15 March 1982.
3. Kline, M. and Kay, I. W., "Electromagnetic Theory and Geometrical Optics," Interscience Publishers, Inc. 1965.
4. Stavroudis, O. N., "The Optics of Rays, Wavefronts, and Caustics," Academic Press, 1972.
5. Struik, D. J., "Differential Geometry," Addison-Wesley Pub. Co., Inc., 1961.
6. Berry, M. V. and Upstill, C., "Catastrophic Optics: Morphologies of Caustics and their Diffraction Patterns," E. Wolf, *Progress in Optics*, XVIII, North-Holland, 1980.
7. Pogorelov, A. V., "Differential Geometry," Noordhoff, N. V.
8. Lipschutz, M. M., "Differential Geometry," McGraw-Hill Book Co., 1969.
9. Stalzer, H. J., Jr., "Comment on the Caustic Curve of a Parabola," *Applied Optics*, 4(9), September 1965.
10. Scarborough, J. B., "The Caustic Curve of an Off-Axis Parabola," *Applied Optics*, 3(12), December 1964.
11. Shealy, D. L. and Burkhard, D. G., "Caustic Surfaces and Irradiance for Reflection and Refraction from an Ellipsoid, Elliptic Paraboloid, and Elliptic Cone," *Applied Optics*, Vol. 12, No. 12, December 1973.
12. Burkhard, D. G. and Shealy, D. L., "Flux Density for Ray Propagation in Geometrical Optics," *Journal of the Optical Society of America*, Vol. 63, No. 3, March 1973.
13. Shealy, D. L. and Burkhard, D. G., "Flux Density for Ray Propagation in Discrete Media Expressed in Terms of the Intrinsic Geometry of the Deflecting Surface," *Optica Acta*, Vol. 20, No. 4, 1973.
14. Guggenheimer, H. W., "Differential Geometry," Dover Publications, 1977.
15. do Carmo, M. P., "Differential Geometry of Curves and Surfaces," Prentice-Hall, Inc., 1976.
16. Stoker, J. J., "Differential Geometry," Wiley-Interscience, 1969.
17. Schmidt, R. F., "Principal Normal Curvature of Surfaces," TM82102, Goddard Space Flight Center, March 1981.
18. Schmidt, R. F., "The Correction of Aberrations Computed in the Aperture Plane of Multifrequency Microwave Radiometer Antennas," TM86090, Goddard Space Flight Center, May 1984.
19. Parke Mathematical Laboratories, Inc., "Calculation of the Caustic (Focal) Surface when the Reflecting Surface is a Paraboloid of Revolution and the Incoming Rays are Parallel," Contract No. AF 19(122) 484, February 1952.
20. Silver, S., "Microwave Antenna Theory and Design," McGraw-Hill Book Co., Inc., 1949.
21. Bleistein, N., "Mathematical Methods for Wave Phenomena," Academic Press, 1984.
22. Hansen, R. C., "Microwave Scanning Antennas," Vol. I, Academic Press, 1964.
23. Sears, F. W., "Optics," Addison-Wesley Publishing Co., Inc., 1949.
24. Uslenghi, P. L. E., "Electromagnetic Scattering," Academic Press, 1978.
25. Wolf, E. and M. Born, "Principles of Optics," Pergamon Press, 1964.
26. Cornell University, "Scientific Experiments for the Arecibo Radio Observatory," Research Report RS 5, 31 March 1960.
27. Cornell University, "Design Studies for the Arecibo Radio Observatory," Research Report, RS 9, 30 June 1960.
28. Cornell University, "Construction of the Department of Defense Ionospheric Research Facility-11," Research RS 22.
29. Kernweis, N. P. and F. H. Cleveland, "A Line-Source Corrector for Large Spherical Reflectors," Air Force Cambridge Research Laboratories, Microwave Physics Laboratory, AFCRL-67-0142, Paper No. 315.
30. Poston, T. and I. Stewart, "Catastrophe Theory and its Applications," Pittman, 1978.
31. Stamnes, J. J. and B. Spjelkavik, "Evaluation of the field near a cusp of a caustic," *Optica Acta*, Vol. 30, No. 9, 1983.
32. Boivin, A., N. Brousseau, and S. C. Biswas, "Electromagnetic diffraction in the focal region of a wide-angle spherical mirror under oblique illumination: An integral representation of the field," *Optica Acta*, Vol. 25, No. 5, 1978.
33. Ibid, "Formal expansion of the diffraction integrals," *Optica Acta*, Vol. 26, No. 3, 1979.
34. Ibid, "Actual field distribution along the axis," *Optica Acta*, Vol. 26, No. 7, 1979.

**APPENDIX A**  
**Gauss/Seidel Aberrations (Parallel Distortion of Gaussian Wavefront)**

$$x = \sigma \sin \zeta \quad , \quad y = -\sigma \cos \zeta \quad (A-1)$$

$$z = - (c^2 - \sigma^2)^{1/2} \quad \text{(Gaussian Sphere)}$$

$$- \omega_{020} I_2 \quad \text{(axial focus)}$$

$$- \omega_{111} I_3 \quad \text{(transverse focus)}$$

$$- \omega_{040} I_2^2 \quad \text{(spherical)}$$

$$- \omega_{222} I_3^2 \quad \text{(astigmatism)}$$

$$- \omega_{220} I_1 I_2 \quad \text{(field curvature/Petzval)}$$

$$- \omega_{131} I_2 I_3 \quad \text{(coma)}$$

$$- \omega_{311} I_3 I_1 \quad \text{(distortion)} \quad (A-2)$$

where

$$I_1 = h^2 \quad , \quad I_2 = \sigma^2 \quad , \quad I_3 = h \sigma \cos \zeta \quad (A-3)$$

Substituting (A-3) into (A-2), the wavefront z-coordinate is given by

$$z = - (c^2 - \sigma^2)^{1/2} - (\omega_{020}) \sigma^2 - (\omega_{111} h) \sigma \cos \zeta - (\omega_{040}) \sigma^4 - (\omega_{222} h^2) \sigma^2 \cos^2 \zeta$$

$$- (\omega_{220} h^2) \sigma^2 - (\omega_{131} h) \sigma^3 \cos \zeta - (\omega_{311} h^3) \sigma \cos \zeta \quad (A-4)$$

The wavefront tangents are then obtained as

$$\bar{x}_u = [ \sin \zeta, -\cos \zeta, \sigma(c^2 - \sigma^2)^{-1/2} - 2(\omega_{020}) \sigma - (\omega_{111} h) \cos \zeta - 4(\omega_{040}) \sigma^3$$

$$- 2(\omega_{222} h^2) \sigma \cos^2 \zeta - 2(\omega_{220} h^2) \sigma - 3(\omega_{131} h) \sigma^2 \cos \zeta - (\omega_{311} h^3) \cos \zeta ] \quad (A-5)$$

and

$$\bar{x}_v = [ \sigma \cos \zeta, \sigma \sin \zeta, (\omega_{111} h) \sigma \sin \zeta + 2(\omega_{222} h^2) \sigma^2 \cos \zeta \sin \zeta$$

$$+ (\omega_{131} h) \sigma^3 \sin \zeta + (\omega_{311} h^3) \sigma \sin \zeta ] \quad (A-6)$$

The second partial derivatives are

$$\bar{x}_{uu} = [ 0, 0, \sigma^2 (c^2 - \sigma^2)^{-3/2} + (c^2 - \sigma^2)^{-1/2} - 2(\omega_{020}) - 12(\omega_{040}) \sigma^2$$

$$- 2(\omega_{222} h^2) \cos^2 \zeta - 2(\omega_{220} h^2) - 6(\omega_{131} h) \sigma \cos \zeta ] \quad (A-7)$$

$$\bar{x}_{uv} = [ \cos \zeta, \sin \zeta, (\omega_{111} h) \sin \zeta + 4(\omega_{222} h^2) \sigma \sin \zeta \cos \zeta + 3(\omega_{131} h) \sigma^2 \sin \zeta$$

$$+ (\omega_{311} h^3) \sin \zeta ] \quad (A-8)$$

$$\bar{x}_{vv} = [ -\sigma \sin \zeta, \sigma \cos \zeta, (\omega_{111} h) \sigma \cos \zeta + 2(\omega_{222} h^2) \sigma^2 (\cos^2 \zeta - \sin^2 \zeta)$$

$$+ (\omega_{131} h) \sigma^3 \cos \zeta + (\omega_{311} h^3) \sigma \cos \zeta ] \quad (A-9)$$

**APPENDIX B**  
**Gauss/Seidel Aberrations (Normal Distortion of Gaussian Wavefront)**

$$\bar{N}_s = - [ \sigma \sin \zeta, - \sigma \cos \zeta, - (c^2 - \sigma^2)^{1/2} ] / c \quad (\text{B-1})$$

is taken as the normal to the Gaussian sphere of radius (c). The wavefront coordinates are given by

$$\begin{aligned} x = & \sigma \sin \zeta + \frac{(\omega_{020})}{c} \sigma^3 \sin \zeta + \frac{(\omega_{111})}{c} h \sigma^2 \sin \zeta \cos \zeta + \frac{(\omega_{040})}{c} \sigma^5 \sin \zeta \\ & + \frac{(\omega_{222})}{c} h^2 \sigma^3 \sin \zeta \cos^2 \zeta + \frac{(\omega_{220})}{c} h^2 \sigma^3 \sin \zeta + \frac{(\omega_{131})}{c} h \sigma^4 \sin \zeta \cos \zeta \\ & + \frac{(\omega_{311})}{c} h^3 \sigma^2 \sin \zeta \cos \zeta \end{aligned} \quad (\text{B-2})$$

$$\begin{aligned} y = & - \sigma \cos \zeta - \frac{(\omega_{020})}{c} \sigma^3 \cos \zeta - \frac{(\omega_{111})}{c} h \sigma^2 \cos^2 \zeta - \frac{(\omega_{040})}{c} \sigma^5 \cos \zeta \\ & - \frac{(\omega_{222})}{c} h^2 \sigma^3 \cos^3 \zeta - \frac{(\omega_{220})}{c} h^2 \sigma^3 \cos \zeta \\ & - \frac{(\omega_{131})}{c} h \sigma^4 \cos^2 \zeta - \frac{(\omega_{311})}{c} h^3 \sigma^2 \cos^2 \zeta \end{aligned} \quad (\text{B-3})$$

$$\begin{aligned} z = & - (c^2 - \sigma^2)^{1/2} - \frac{(\omega_{020})}{c} \sigma^2 (c^2 - \sigma^2)^{1/2} - \frac{(\omega_{111})}{c} h \sigma (c^2 - \sigma^2)^{1/2} \cos \zeta \\ & - \frac{(\omega_{040})}{c} \sigma^4 (c^2 - \sigma^2)^{1/2} - \frac{(\omega_{222})}{c} h^2 \sigma^2 (c^2 - \sigma^2)^{1/2} \cos^2 \zeta \\ & - \frac{(\omega_{220})}{c} h^2 \sigma^2 (c^2 - \sigma^2)^{1/2} - \frac{(\omega_{131})}{c} h \sigma^3 (c^2 - \sigma^2)^{1/2} \cos \zeta \\ & - \frac{(\omega_{311})}{c} h^3 \sigma^1 (c^2 - \sigma^2)^{1/2} \cos \zeta \end{aligned} \quad (\text{B-4})$$

The wavefront tangents are then obtained as

$$\begin{aligned} \bar{x}_u = & \left[ \sin \zeta + 3 \frac{(\omega_{020})}{c} \sigma^2 \sin \zeta + 2 \frac{(\omega_{111})}{c} h \sigma \sin \zeta \cos \zeta + 5 \frac{(\omega_{040})}{c} \sigma^4 \sin \zeta \right. \\ & + 3 \frac{(\omega_{222})}{c} h^2 \sigma^2 \sin \zeta \cos^2 \zeta + 3 \frac{(\omega_{220})}{c} h^2 \sigma^2 \sin \zeta + 4 \frac{(\omega_{131})}{c} h \sigma^3 \sin \zeta \cos \zeta \\ & \left. + 2 \frac{(\omega_{311})}{c} h^3 \sigma \sin \zeta \cos \zeta \right] \hat{i} + \end{aligned} \quad (\text{B-5})$$

$$\left[ -\cos \zeta - \frac{3(\omega_{020})}{c} \sigma^2 \cos \zeta - \frac{2(\omega_{111})}{c} h \sigma \cos^2 \zeta - \frac{5(\omega_{040})}{c} \sigma^4 \cos \zeta \right. \\ \left. - \frac{3(\omega_{222})}{c} h^2 \sigma^2 \cos^3 \zeta - \frac{3(\omega_{220})}{c} h^2 \sigma^2 \cos \zeta - \frac{4(\omega_{131})}{c} h \sigma^3 \cos^2 \zeta \right. \\ \left. - \frac{2(\omega_{311})}{c} h^3 \sigma \cos^2 \zeta \right] \hat{j} +$$

$$\left[ \sigma (c^2 - \sigma^2)^{-1/2} + \frac{(\omega_{020})}{c} \sigma^3 (c^2 - \sigma^2)^{-1/2} - \frac{2(\omega_{020})}{c} \sigma (c^2 - \sigma^2)^{1/2} \right. \\ + \frac{(\omega_{111})}{c} h \cos \zeta \sigma^2 (c^2 - \sigma^2)^{-1/2} - \frac{(\omega_{111})}{c} h \cos \zeta (c^2 - \sigma^2)^{1/2} \\ + \frac{(\omega_{040})}{c} \sigma^5 (c^2 - \sigma^2)^{-1/2} - \frac{4(\omega_{040})}{c} \sigma^3 (c^2 - \sigma^2)^{1/2} \\ + \frac{(\omega_{222})}{c} h^2 \cos^2 \zeta \sigma^3 (c^2 - \sigma^2)^{-1/2} - \frac{2(\omega_{222})}{c} h^2 \cos^2 \zeta \sigma (c^2 - \sigma^2)^{1/2} \\ + \frac{(\omega_{220})}{c} h^2 \sigma^3 (c^2 - \sigma^2)^{-1/2} - \frac{2(\omega_{220})}{c} h^2 \sigma (c^2 - \sigma^2)^{1/2} \\ + \frac{(\omega_{131})}{c} h \cos \zeta \sigma^4 (c^2 - \sigma^2)^{-1/2} - \frac{3(\omega_{131})}{c} h \cos \zeta \sigma^2 (c^2 - \sigma^2)^{1/2} \\ \left. + \frac{(\omega_{311})}{c} h^3 \cos \zeta \sigma^2 (c^2 - \sigma^2)^{-1/2} - \frac{(\omega_{311})}{c} h^3 \cos \zeta (c^2 - \sigma^2)^{1/2} \right] \hat{k}$$

(B-5)

$$\bar{x}_v = \left[ \sigma \cos \zeta + \frac{(\omega_{020})}{c} \sigma^3 \cos \zeta + \frac{(\omega_{111})}{c} h \sigma^2 (\cos^2 \zeta - \sin^2 \zeta) + \frac{(\omega_{040})}{c} \sigma^5 \cos \zeta \right. \\ \left. + \frac{(\omega_{222})}{c} h^2 \sigma^3 (\cos^3 \zeta - 2 \sin^2 \zeta \cos \zeta) + \frac{(\omega_{220})}{c} h^2 \sigma^3 \cos \zeta \right. \\ \left. + \frac{(\omega_{131})}{c} h \sigma^4 (\cos^2 \zeta - \sin^2 \zeta) + \frac{(\omega_{311})}{c} h^3 \sigma^2 (\cos^2 \zeta - \sin^2 \zeta) \right] \hat{i} +$$

$$\left[ \sigma \sin \zeta + \frac{(\omega_{020})}{c} \sigma^3 \sin \zeta + \frac{2(\omega_{111})}{c} h \sigma^2 \sin \zeta \cos \zeta + \frac{(\omega_{040})}{c} \sigma^5 \sin \zeta \right. \\ \left. + \frac{3(\omega_{222})}{c} h^2 \sigma^3 \sin \zeta \cos^2 \zeta + \frac{(\omega_{220})}{c} h^2 \sigma^3 \sin \zeta \right]$$

(B-6)

$$\begin{aligned}
& + \frac{2(\omega_{131} h)}{c} \sigma^4 \sin \zeta \cos \zeta + \frac{2(\omega_{311} h^3)}{c} \sigma^2 \sin \zeta \cos \zeta \Big] \hat{j} + \\
& \left[ \frac{(\omega_{111} h)}{c} \sigma (c^2 - \sigma^2)^{1/2} \sin \zeta + \frac{2(\omega_{222} h^2)}{c} \sigma^2 (c^2 - \sigma^2)^{1/2} \sin \zeta \cos \zeta \right. \\
& \left. + \frac{(\omega_{131} h)}{c} \sigma^3 (c^2 - \sigma^2)^{1/2} \sin \zeta + \frac{(\omega_{311} h^3)}{c} \sigma (c^2 - \sigma^2)^{1/2} \sin \zeta \right] \hat{k} \quad (\text{B-6})
\end{aligned}$$

The second partial derivatives are

$$\begin{aligned}
\bar{x}_{uu} = & \left[ \frac{6(\omega_{020})}{c} \sigma \sin \zeta + \frac{2(\omega_{111} h)}{c} \sin \zeta \cos \zeta + \frac{20(\omega_{040})}{c} \sigma^3 \sin \zeta + \frac{6(\omega_{222} h^2)}{c} \sigma \sin \zeta \cos^2 \zeta \right. \\
& \left. + \frac{6(\omega_{220} h^2)}{c} \sigma \sin \zeta + \frac{12(\omega_{131} h)}{c} \sigma^2 \sin \zeta \cos \zeta + \frac{2(\omega_{311} h^3)}{c} \sin \zeta \cos \zeta \right] \hat{i} + \\
& \left[ \frac{-6(\omega_{020})}{c} \sigma \cos \zeta - \frac{2(\omega_{111} h)}{c} \cos^2 \zeta - \frac{20(\omega_{040})}{c} \sigma^3 \cos \zeta - \frac{6(\omega_{222} h^2)}{c} \sigma \cos^3 \zeta \right. \\
& \left. - \frac{6(\omega_{220} h^2)}{c} \sigma \cos \zeta - \frac{12(\omega_{131} h)}{c} \sigma^2 \cos^2 \zeta - \frac{2(\omega_{131} h^3)}{c} \cos^2 \zeta \right] \hat{j} + \\
& \left[ \sigma^2 (c^2 - \sigma^2)^{-3/2} + (c^2 - \sigma^2)^{-1/2} + \frac{(\omega_{020})}{c} \sigma^4 (c^2 - \sigma^2)^{-3/2} + \frac{3(\omega_{020})}{c} \sigma^2 (c^2 - \sigma^2)^{-1/2} \right. \\
& + \frac{2(\omega_{020})}{c} \sigma^2 (c^2 - \sigma^2)^{-1/2} - \frac{2(\omega_{020})}{c} (c^2 - \sigma^2)^{-1/2} \\
& + \frac{(\omega_{111} h)}{c} \sigma^3 (c^2 - \sigma^2)^{-3/2} \cos \zeta + \frac{2(\omega_{111} h)}{c} \sigma (c^2 - \sigma^2)^{-1/2} \cos \zeta \\
& + \frac{(\omega_{111} h)}{c} \sigma (c^2 - \sigma^2)^{-1/2} \cos \zeta \\
& + \frac{(\omega_{040})}{c} \sigma^6 (c^2 - \sigma^2)^{-3/2} + \frac{5(\omega_{040})}{c} \sigma^4 (c^2 - \sigma^2)^{-1/2} \\
& + \frac{4(\omega_{040})}{c} \sigma^4 (c^2 - \sigma^2)^{-1/2} - \frac{12(\omega_{040})}{c} \sigma^2 (c^2 - \sigma^2)^{1/2} \\
& \left. + \frac{(\omega_{222} h^2)}{c} \sigma^4 (c^2 - \sigma^2)^{-3/2} \cos^2 \zeta + \frac{3(\omega_{222} h^2)}{c} \sigma^2 (c^2 - \sigma^2)^{-1/2} \cos^2 \zeta \right] \quad (\text{B-7})
\end{aligned}$$

$$\begin{aligned}
& + \frac{2(\omega_{222} h^2)}{c} \sigma^2 (c^2 - \sigma^2)^{-1/2} \cos^2 \zeta - \frac{2(\omega_{222} h^2)}{c} (c^2 - \sigma^2)^{1/2} \cos^2 \zeta \\
& + \frac{(\omega_{220} h^2)}{c} \sigma^4 (c^2 - \sigma^2)^{-3/2} + \frac{3(\omega_{220} h^2)}{c} \sigma^2 (c^2 - \sigma^2)^{-1/2} \\
& + \frac{2(\omega_{220} h^2)}{c} \sigma^2 (c^2 - \sigma^2)^{-1/2} - \frac{2(\omega_{220} h^2)}{c} (c^2 - \sigma^2)^{1/2} \\
& + \frac{(\omega_{131} h)}{c} \sigma^5 (c^2 - \sigma^2)^{-3/2} \cos \zeta + \frac{4(\omega_{131} h)}{c} \sigma^3 (c^2 - \sigma^2)^{-1/2} \cos \zeta \\
& + \frac{3(\omega_{131} h)}{c} \sigma^3 (c^2 - \sigma^2)^{-1/2} \cos \zeta - \frac{6(\omega_{131} h)}{c} \sigma (c^2 - \sigma^2)^{1/2} \cos \zeta \\
& + \left. \frac{(\omega_{311} h^3)}{c} \sigma^3 (c^2 - \sigma^2)^{-3/2} \cos \zeta + \frac{3(\omega_{311} h^3)}{c} \sigma (c^2 - \sigma^2)^{-1/2} \cos \zeta \right] \hat{k} \quad (B-7)
\end{aligned}$$

$\bar{x}_{uv} =$

$$\begin{aligned}
& \left[ \cos \zeta + \frac{3(\omega_{020})}{c} \sigma^2 \cos \zeta + \frac{2(\omega_{111} h)}{c} \sigma (\cos^2 \zeta - \sin^2 \zeta) + \frac{5(\omega_{040})}{c} \sigma^4 \cos \zeta \right. \\
& + \frac{3(\omega_{222} h^2)}{c} \sigma^2 (\cos^3 \zeta - 2 \sin^2 \zeta \cos \zeta) + \frac{3(\omega_{220} h^2)}{c} \sigma^2 \cos \zeta \\
& \left. + \frac{4(\omega_{131} h)}{c} \sigma^3 (\cos^2 \zeta - \sin^2 \zeta) + \frac{2(\omega_{311} h^3)}{c} \sigma (\cos^2 \zeta - \sin^2 \zeta) \right] \hat{i} +
\end{aligned}$$

$$\begin{aligned}
& \left[ \sin \zeta + \frac{3(\omega_{020})}{c} \sigma^2 \sin \zeta + \frac{4(\omega_{111} h)}{c} \sigma \sin \zeta \cos \zeta + \frac{5(\omega_{040})}{c} \sigma^4 \sin \zeta \right. \\
& + \frac{9(\omega_{222} h^2)}{c} \sigma^2 \sin \zeta \cos^2 \zeta + \frac{3(\omega_{220} h^2)}{c} \sigma^2 \sin \zeta \\
& \left. + \frac{8(\omega_{131} h)}{c} \sigma^3 \sin \zeta \cos \zeta + \frac{4(\omega_{311} h^3)}{c} \sigma \sin \zeta \cos \zeta \right] \hat{j} +
\end{aligned}$$

$$\begin{aligned}
& \left[ - \frac{(\omega_{111} h)}{c} \sin \zeta \sigma^2 (c^2 - \sigma^2)^{-1/2} + \frac{(\omega_{111} h)}{c} \sin \zeta (c^2 - \sigma^2)^{1/2} \right. \\
& - \frac{2(\omega_{222} h^2)}{c} \sigma^3 (c^2 - \sigma^2)^{-1/2} \sin \zeta \cos \zeta + \frac{4(\omega_{222} h^2)}{c} \sigma (c^2 - \sigma^2)^{1/2} \sin \zeta \cos \zeta \\
& \left. - \frac{(\omega_{131} h)}{c} \sigma^4 (c^2 - \sigma^2)^{-1/2} \sin \zeta + \frac{3(\omega_{131} h)}{c} \sigma^2 (c^2 - \sigma^2)^{1/2} \sin \zeta \right] \quad (B-8)
\end{aligned}$$

$$- \frac{(\omega_{311} h^3) \sigma^2 (c^2 - \sigma^2)^{-1/2} \sin \zeta + (\omega_{311} h^3) (c^2 - \sigma^2)^{1/2} \sin \zeta}{c} \Big] \hat{k} \quad (\text{B-8})$$

$\bar{x}_{\text{vw}} =$

$$\begin{aligned} & \left[ -\sigma \sin \zeta - \frac{(\omega_{020}) \sigma^3 \sin \zeta - 4(\omega_{111} h) \sigma^2 \sin \zeta \cos \zeta - (\omega_{040}) \sigma^5 \sin \zeta}{c} \right. \\ & + \frac{(\omega_{222} h^2) \sigma^3 (2 \sin^3 \zeta - 7 \sin \zeta \cos^2 \zeta - (\omega_{220} h^2) \sigma^3 \sin \zeta}{c} \\ & \left. + \frac{(\omega_{131} h) \sigma^4 (-4 \sin \zeta \cos \zeta) - (\omega_{311} h^3) \sigma^2 (4 \sin \zeta \cos \zeta)}{c} \right] \hat{i} + \end{aligned}$$

$$\begin{aligned} & \left[ \sigma \cos \zeta + \frac{(\omega_{020}) \sigma^3 \cos \zeta + 2(\omega_{111} h) \sigma^2 (\cos^2 \zeta - \sin^2 \zeta) + (\omega_{040}) \sigma^5 \cos \zeta}{c} \right. \\ & + 3 \frac{(\omega_{222} h^2) \sigma^3 (\cos^3 \zeta - 2 \sin^2 \zeta \cos \zeta + (\omega_{220} h^2) \sigma^3 \cos \zeta}{c} \\ & \left. + 2 \frac{(\omega_{131} h) \sigma^4 (\cos^2 \zeta - \sin^2 \zeta) + 2(\omega_{311} h^3) \sigma^2 (\cos^2 \zeta - \sin^2 \zeta)}{c} \right] \hat{j} + \end{aligned}$$

$$\begin{aligned} & \left[ \frac{(\omega_{111} h) \sigma (c^2 - \sigma^2)^{1/2} \cos \zeta + 2(\omega_{222} h^2) \sigma^2 (c^2 - \sigma^2)^{1/2} (\cos^2 \zeta - \sin^2 \zeta)}{c} \right. \\ & \left. + \frac{(\omega_{131} h) \sigma^3 (c^2 - \sigma^2)^{1/2} \cos \zeta + (\omega_{311} h^3) \sigma (c^2 - \sigma^2)^{1/2} \cos \zeta}{c} \right] \hat{k} \quad (\text{B-9}) \end{aligned}$$

## APPENDIX C

### The Caustic Surfaces of a Paraboloid and Inclined Plane Wave

A complete verification of the caustic equation obtained in Ref. 19 for the paraboloid and inclined plane wave is tedious. Some of the important factors are given here for convenience, together with the final result. In Ref. 19, the parametric equations of the reflector surface are given as

$$x_1 = \frac{1}{4a} (\rho^2 - 4a^2) \quad (\text{C-1})$$

$$x_2 = \rho \cos \theta \quad (\text{C-2})$$

$$x_3 = \rho \sin \theta \quad (\text{C-3})$$

The details pertaining to the reflected ray are omitted entirely here since they are easily obtained from

$$\bar{S}_r = \bar{S}_i - 2(\bar{N} \cdot \bar{S}_i) \bar{N} \quad (\text{C-4})$$

The components of a reflected unit vector are

$$\begin{aligned} \bar{S}_r = X_i = (X_1, X_2, X_3) = & \\ & \left( \frac{8a^2 \cos \varphi - 4a \rho \sin \theta \sin \varphi}{4a^2 + \rho^2} - \cos \varphi \right) \hat{i} + \\ & \left( \frac{-4a \rho \cos \theta \cos \varphi + 2 \rho^2 \sin \theta \cos \theta \sin \varphi}{4a^2 + \rho^2} \right) \hat{j} + \\ & \left( \frac{-4a \rho \sin \theta \cos \varphi + 2 \rho^2 \sin^2 \theta \sin \varphi}{4a^2 + \rho^2} \right) \hat{k} + \end{aligned} \quad (\text{C-5})$$

From the preceding  $X_i$ , the partial derivatives

$$\begin{aligned} \frac{\partial X_i}{\partial u_1} = \frac{\partial X_i}{\partial \rho} = & \frac{4a \cos \varphi}{(4a^2 + \rho^2)^2} (\rho^2 \sin \theta \tan \varphi - 4a \rho - 4a^2 \sin \theta \tan \varphi) \hat{i} + \\ & \frac{4a \cos \varphi}{(4a^2 + \rho^2)^2} (\rho^2 \cos \theta + 4a \rho \sin \theta \cos \theta \tan \varphi - 4a^2 \cos \theta) \hat{j} + \\ & \frac{4a \cos \varphi}{(4a^2 + \rho^2)^2} (\rho^2 \sin \theta + 4a \rho \sin^2 \theta \tan \varphi - 4a^2 \sin \theta) \hat{k} \end{aligned} \quad (\text{C-6})$$

and

$$\begin{aligned} \frac{\partial X_1}{\partial u_2} = \frac{\partial X_1}{\partial \theta} &= \frac{-4a \rho \cos \theta \sin \varphi}{4a^2 + \rho^2} \hat{i} + \\ &\frac{\rho \cos \varphi}{4a^2 + \rho^2} (4a \sin \theta + 2 \rho \cos 2 \theta \tan \varphi) \hat{j} + \\ &\frac{\rho \cos \varphi}{4a^2 + \rho^2} (-4a \cos \theta + 2 \rho \sin 2 \theta \tan \varphi) \hat{k} + \end{aligned} \quad (C-7)$$

give

$$G_{11} = 16a^2(\cos^2 \varphi + \sin^2 \theta \sin^2 \varphi) / (4a^2 + \rho^2)^2 \quad (C-8)$$

$$G_{12} = G_{21} = 8a \rho \cos \theta \sin \varphi (\rho \cos \varphi + 2a \sin \theta \sin \varphi) / (4a^2 + \rho^2)^2 \quad (C-9)$$

$$G_{22} = 4\rho^2 [4a^2 + \rho^2 - (2a \sin \theta \sin \varphi - \rho \cos \varphi)^2] / (4a^2 + \rho^2)^2 \quad (C-10)$$

The reflector tangents

$$\frac{\partial x_i}{\partial u_1} = \frac{\partial x_i}{\partial \rho} = \frac{\rho}{2a} \hat{i} + \cos \theta \hat{j} + \sin \theta \hat{k} \quad (C-11)$$

$$\frac{\partial x_i}{\partial u_2} = \frac{\partial x_i}{\partial \theta} = -\rho \sin \theta \hat{j} + \rho \cos \theta \hat{k} \quad (C-12)$$

together with the partial derivations of  $X_i$ , give

$$g_{11} = 2(\rho \sin \theta \sin \varphi - 2a \cos \varphi) / (4a^2 + \rho^2) \quad (C-13)$$

$$g_{12} = g_{21} = 0 \quad (C-14)$$

$$g_{22} = 2\rho^2(\rho \sin \theta \sin \varphi - 2a \cos \varphi) / (4a^2 + \rho^2) \quad (C-15)$$

The equation for the coordinates of the caustic surfaces of the paraboloid with incident plane wave inclined at an angle ( $\varphi$ ) is obtained as

$$\begin{aligned} \bar{x}_i = x_1 + &\left[ 1 - \frac{(2a + x_1) \cos \varphi}{(2a \cos \varphi - x_3 \sin \varphi)} \right] Q \hat{i} + \\ &\left[ x_2 - \frac{x_2}{2a} \right] Q \hat{j} + \left[ x_3 - \frac{x_3}{2a} - \frac{(2a + x_1) \sin \varphi}{(2a \cos \varphi - x_3 \sin \varphi)} \right] Q \hat{k} \end{aligned} \quad (C-16)$$

where

$$Q = 2a + x_1 - \cos \varphi (x_1 \cos \varphi + x_3 \sin \varphi) \pm (2a + x_1) \sin \varphi \sqrt{1 - \left( \frac{x_1 \cos \varphi + x_3 \sin \varphi}{2a + x_1} \right)^2} \quad (C-17)$$

and the point  $(x_1, x_2, x_3)$  lies on the paraboloid.



# Report Documentation Page

1. Report No. <b>NASA TM-87805</b>		2. Government Accession No.		3. Recipient's Catalog No.	
4. Title and Subtitle <b>Analytical Caustic Surfaces</b>				5. Report Date <b>April 1987</b>	
				6. Performing Organization Code <b>675.0</b>	
7. Author(s) <b>R. F. Schmidt</b>				8. Performing Organization Report No. <b>87BO244</b>	
				10. Work Unit No.	
9. Performing Organization Name and Address <b>Telecommunications Branch Networks Division Goddard Space Flight Center</b>				11. Contract or Grant No.	
				13. Type of Report and Period Covered <b>Technical Memorandum</b>	
12. Sponsoring Agency Name and Address <b>National Aeronautics and Space Administration Washington, D.C. 20546-0001</b>				14. Sponsoring Agency Code <b>531.2</b>	
				15. Supplementary Notes	
16. Abstract <p>This document discusses the determination of caustic surfaces in terms of rays, reflectors and wavefronts. Analytical caustics are obtained as a family of lines, a set of points, and several types of equations for geometries encountered in optics and microwave applications. Standard methods of differential geometry are applied under different approaches: directly to reflector surfaces, and alternatively, to wavefronts, to obtain analytical caustics of two sheets or branches. Gauss/Seidel aberrations are introduced into the wavefront approach, forcing the retention of all three coefficients of both the first and the second – fundamental forms of differential geometry. An existing method for obtaining caustic surfaces through exploitation of the singularities in flux density is examined, and several constant-intensity contour maps are developed using only the intrinsic Gaussian, mean, and normal curvatures of the reflector. Numerous references are provided for extending the material of the present document to the morphologies of caustics and their associated diffraction patterns.</p>					
17. Key Words (Suggested by Author(s)) <b>Analytical Caustics, Center Surfaces, Focal Regions, Microwave Antennas</b>			18. Distribution Statement <b>Unlimited–Unclassified</b>  <b>Subject Category–33</b>		
19. Security Classif. (of this report) <b>Unclassified</b>		20. Security Classif. (of this page) <b>Unclassified</b>		21. No. of pages	22. Price